Theses and Dissertations

1972

Transmission cavity stabilization of microwave oscillators

Dennis Eugene White
Lehigh University

Follow this and additional works at: https://preserve.lehigh.edu/etd

Part of the Electrical and Computer Engineering Commons

Transmission Cavity Stabilization of Microwave Oscillators
Dennis Eugene White

ABSTRACT

A theoretical analysis of cavity stabilization of microwave oscillators is presented. The stabilizing system which consists of a length of transmission line, a lumped conductance and a high Q transmission cavity, is characterized by an equivalent circuit which permits a substantial portion of the analysis to be performed using lumped element circuit considerations. The stabilization factor, admittance presented to the oscillator, and insertion loss of the system are determined from the parameters of this equivalent circuit.

Suppression of extraneous modes of oscillation is also considered. The use of a shunt conductance to achieve this suppression is discussed along with the effects of this technique on stabilization factor and tuning range.

Design equations, for optimum loading of the oscillator and for maximization of tuning range, are presented along with experimental results for an X-band IMPATT oscillator, stabilized by a high Q transmission cavity.

TRANSMISSION CAVITY

STABILIZATION OF

MICROWAVE OSCILLATORS

by

Dennis Eugene White

A Thesis

Presented to the Graduate Committee

of Lehigh University

in Candidacy for the Degree of

Master of Science

in Electrical Engineering

Lehigh University

1972

This thesis is accepted and approved in partial fulfill-
ment of the requirements for the degree of Master of Science.

17 MAY 1972
(Date)

John Andria
Professor in Charge

_AK_
Chairman of Department

ACKNOWLEDGEMENTS

LIST OF FIGURES

TABLE OF CONTENTS

ABSTRACT

A theoretical analysis of cavity stabilization of micro-
wave oscillators is presented. The stabilizing system which
consists of a length of transmission line, a lumped conduct-
ance and a high Q transmission cavity, is characterized by an
equivalent circuit which permits a substantial portion of the
analysis to be performed using lumped element circuit consid-
erations. The stabilization factor, admittance presented to
the oscillator, and insertion loss of the system are deter-
mined from the parameters of this equivalent circuit.

Suppression of extraneous modes of oscillation is also
considered. The use of a shunt conductance to achieve this
suppression is discussed along with the effects of this tech-
nique on stabilization factor and tuning range.

Design equations, for optimum loading of the oscillator
and for maximization of tuning range, are presented along
with experimental results for an X-band IMPATT oscillator,
stabilized by a high Q transmission cavity.

INTRODUCTION

Microwave oscillators are in general subject to frequency perturbations of two general types. Frequency modulation or phase noise is comprised of random short term frequency variations which can be characterized in terms of modulation rates in the video frequency range; while frequency drift describes changes in operating frequency over extended periods of time.

Another property of microwave oscillators is a dependence of operating frequency upon reactive loading, or frequency pulling. In practice, this effect is often eliminated by isolating the source from the load. It has been shown [1], however, that dependence of operating frequency upon loading can be exploited in reducing the frequency perturbations described above.

Qualitatively, a significant degree of stabilization is possible when a change in susceptance with frequency much greater than that of the oscillator is exhibited by the load. In the microwave frequency range, large changes in susceptance with frequency are inherent in a high Q cavity structure.

In general, the oscillator must be coupled to the stabilizing cavity through a length of transmission line measuring at least one half wavelength. This section of line can itself act as a resonator, introducing extraneous modes of oscillation.

A shunt conductance, placed midway between the source and stabilizing cavity can be used to eliminate such modes but simultaneously degrades system performance. Specifically, both tuning range and stabilization factor can be significantly reduced by excessively large values of shunt conductance.

This analysis includes a derivation of the minimum conductance required to guarantee mode suppression. It is further shown that for practical systems, there exists an optimum conductance value which maximizes tuning range while introducing a small additional degradation of stabilization factor relative to that produced by the minimum allowable conductance.

I. STABILIZING ACTION

I-1. STABILIZATION FACTOR

The stabilization factor, S, is by definition the ratio of frequency shift induced in a free running oscillator by some perturbation, to the frequency shift induced by applying that same perturbation to the oscillator loaded by a stabilization network.

The susceptance functions of the oscillator and load, B_{OSC} and B_L respectively, are used to compute S. At the free running frequency, ω_0, the oscillator susceptance is zero. If it is assumed that B_L also exhibits a zero crossing at ω_0 and that B_L and B_{OSC} are linear functions of frequency then,

$$B_{OSC} = \frac{dB_{OSC}}{d\omega} (\omega - \omega_0) \tag{1a}$$

and

$$B_L = \frac{dB_L}{d\omega} (\omega - \omega_0). \tag{1b}$$

The introduction of some perturbation which shifts the free running frequency to $\omega_0' = \omega_0 + \Delta\omega_{FR}$, produces the modified susceptance function,

$$B_{OSC}' = \frac{dB_{OSC}}{d\omega} [\omega - (\omega_0 + \Delta\omega_{FR})].$$

The corresponding frequency shift, $\Delta\omega_S$, induced in the reactively loaded oscillator is obtained from the condition:

$$B'_{OSC} + B_L = 0 \text{ at } \omega = \omega_0 + \Delta\omega_S,$$

from which,

$$\frac{dB_{OSC}}{d\omega}\left[(\omega_0 + \Delta\omega_S) - (\omega_0 + \Delta\omega_{FR})\right] = -\frac{dB_L}{d\omega}\left[(\omega_0 + \Delta\omega_S) - \omega_0\right].$$

Rearranging,

$$\frac{\Delta\omega_{FR}}{\Delta\omega_S} \triangleq S = 1 + \frac{dB_L/d\omega}{dB_{OSC}/d\omega} \tag{2}$$

which specifies that, given the conditions of Equations (1a) and (1b), the frequency shift, $\Delta\omega_{FR}$, of a free running oscillator is altered through reactive loading by a factor of

$$\left(1 + \frac{dB_L/d\omega}{dB_{OSC}/d\omega}\right)^{-1}.$$

Two special cases are of interest.

Case (1). For $\dfrac{dB_L/d\omega}{dB_{OSC}/d\omega} \gg 1$, the frequency shift $\Delta\omega_{FR}$ is substantially reduced; the desired result in stabilizing systems.

Case (2). For $\dfrac{dB_L/d\omega}{dB_{OSC}/d\omega} < -1$, or $S < 0$, a condition of unstable equilibrium is developed in which oscillations will not build up. Therefore, resonant frequencies exhibiting $S < 0$ may be ignored.

Hence, effective stabilization systems must exhibit a large positive change of susceptance with frequency in the neighborhood of their operating frequency.

I.2. STABILIZATION SYSTEM

The desired large value of $dB_L/d\omega$ can be realized with the stabilizing system shown schematically in Figure 1. A microwave oscillator is coupled through a section of transmission line or waveguide to one port of a high Q transmission cavity, the other port being coupled to the useful load. The simple G-L-C lumped element representations employed in describing the oscillator and stabilizing cavities are valid over a limited frequency range near a particular mode of resonance provided any additional modes are sufficiently removed in frequency. M_{OSC}, M_1 and M_2 are ideal transformers representing the coupling of the two cavities to the adjacent transmission lines, while the detuned short positions, planes A-A and B-B, correspond to reference planes from which their respective cavities appear as simple G-L-C circuits. In general, detuned short planes are physically located very close to their corresponding coupling mechanisms (iris, loop, etc.) [2].

Extraneous modes of oscillation are suppressed by the shunt conductance, G_S. The required value of this element, as a function of $dB_{OSC}/d\omega$ and line length, is determined in Section II. For most practical systems a value lying between 0.04 and 0.25, normalized with respect to the characteristic

admittance of the transmission line, Y_0, is required.

In general, the turns ratios of the coupling transformers (hence G_c', L_c' and C_c') are unknown. However, the normalized admittance of the stabilizing cavity and load, referred to Plane B-B, can be determined from the unloaded quality factor of the stabilizing cavity, Q_0, and the coupling coefficients of ports 1 and 2. The coupling coefficient, β, is defined for each port as the ratio of external to internal losses with a matched load at that port and the coupling at the remaining port set equal to zero. The normalized impedance exhibited by the cavity at resonance, with zero coupling at the remaining port, is also numerically equal to β. Subscripts 1 and 2 refer to the coupling coefficients of the input and output ports respectively.

From the definition of β_2, the load conductance (matched to the line) can be lumped with the internal cavity elements as shown in Figure 2.

Similarly, from the definition of β_1, the equivalent elements of the stabilizing cavity and load, referred to plane B-B, can be determined; cf. Figure 3. Normalized elements $\bar{G}_c$, $\bar{L}_c$ and $\bar{C}_c$ can be expressed in terms of the measurable quantities β_1, β_2, Q_0 and the resonant frequency of the stabilizing cavity, ω_r.

Using the relationship,

$$Q_o = \frac{\omega_r C_c'}{G_c'} = \frac{\omega_r \bar{C}_c}{(1/\beta_1)} = \omega_r \bar{C}_c \beta_1;$$

the normalized elements,

$$\bar{C}_c = \frac{C_c}{Y_o} = \frac{Q_o}{\beta_1 \omega_r}, \tag{3a}$$

$$\bar{L}_c = L_c Y_o = \frac{1}{(\omega_r^2 \bar{C}_c)} = \frac{\beta_1}{\omega_r Q_o}, \tag{3b}$$

and

$$\bar{G}_c = \frac{G_c}{Y_o} = \frac{1+\beta_2}{\beta_1}. \tag{3c}$$

In order to obtain the degree of stabilization provided by the system, the load admittance, Y_L, as a function of frequency, presented to the oscillator at plane A-A must be known. Assuming $\lambda/4 \approx \lambda_r/4$ over a small frequency range near resonance, standard admittance transforming relationships yield,

$$\bar{Y}_L = \frac{Y_L}{Y_o} = \frac{\bar{G}_S[\bar{G}_c^2 + (\omega\bar{C}_c - 1/\omega\bar{L}_c)^2] + \bar{G}_c + j(\omega\bar{C}_c - 1/\omega\bar{L}_c)}{\bar{G}_S^2[\bar{G}_c^2 + (\omega\bar{C}_c - 1/\omega\bar{L}_c)^2] + 2\bar{G}_S\bar{G}_c + 1}. \tag{4}$$

For high Q systems, it is reasonable to assume that changes in the admittance transformation effected by the transmission line with frequency are negligible.

The admittance defined by Equation (4) is identical to that of the circuit shown in Figure 4. The transmission line and shunt conductance may therefore be replaced by a series

resistance whose normalized <u>resistance</u> value, $\bar{R}'_S$, is numerically equal to the normalized <u>conductance</u>, $\bar{G}_S$. This equivalent circuit simplifies the analysis near resonance in that standard lumped element circuit theory can be applied to the stabilizing network.

Separating the real and imaginary parts of $\bar{Y}_L = \bar{G}_L + j\bar{B}_L$,

$$\bar{G}_L = \frac{\bar{G}_S[\bar{G}_C^2 + (\omega\bar{C}_C - 1/\omega\bar{L}_C)^2] + \bar{G}_C}{\bar{G}_S^2[\bar{G}_C^2 + (\omega\bar{C}_C - 1/\omega\bar{L}_C)^2] + 2\bar{G}_S\bar{G}_C + 1} \tag{5a}$$

and

$$\bar{B}_L = \frac{\omega\bar{C}_C - 1/\omega\bar{L}_C}{\bar{G}_S^2[\bar{G}_C^2 + (\omega\bar{C}_C - 1/\omega\bar{L}_C)^2] + 2\bar{G}_S\bar{G}_C + 1}. \tag{5b}$$

At resonance the load conductance,

$$\bar{G}_L(\text{resonance}) = \frac{1}{\bar{G}_S + 1/\bar{G}_C},$$

which is just the series combination of $\bar{R}'_S$ and $1/\bar{G}_C$. Away from resonance, the stabilizing cavity admittance rapidly approaches infinity yielding,

$$\bar{G}_L(\text{detuned}) \approx 1/\bar{G}_S.$$

The load susceptance, B_L, near resonance is a more complicated function of frequency. Unlike the susceptance function of the stabilizing cavity alone, B_L is not a monotonically increasing function of frequency but exhibits local extrema above and below resonance. Figures 5a and 5b are plots of the conductance and susceptance functions respectively for a typical stabilizing system having parameters Q_o = 10,000, β_1 = 1.0, β_2 = 0.25, $\bar{G}_S$ = 0.2 and line length 2ℓ = $\lambda r/2$.

These plots, which include the effect of the changing electrical length of the transmission line, are in excellent agreement with Equations (5a) and (5b) near ω_r. In Figure 5b, the <u>negative</u> of the susceptance function of a typical oscillator exhibiting $\omega_o = \omega_r$ and $\frac{d\bar{B}_{OSC}}{d\omega/\omega_o} = 500$ is also plotted and used below.

At $\omega = \omega_r$, the change in load susceptance with frequency is, from Equation (5b),

$$\left.\frac{d\bar{B}_L}{d\omega/\omega_r}\right|_{\omega_r} = \frac{(\bar{G}_S^2\bar{G}_C^2+2\bar{G}_S\bar{G}_C+1)2\bar{C}_C}{(\bar{G}_S^2\bar{G}_C^2+2\bar{G}_S\bar{G}_C+1)^2} = \frac{2\bar{C}_C}{(\bar{G}_S\bar{G}_C+1)^2} \qquad (6)$$

which corresponds to a decrease in the influence of the stabilizing cavity by a factor of $(\bar{G}_S\bar{G}_C + 1)^{-2}$. For this reason, unnecessarily large values of $\bar{G}_S$ must be avoided.

The susceptance change with frequency exhibited by an oscillator can be determined from a measure of the pulling

factor, L, which by definition is the total frequency shift, expressed in Hz, induced in an oscillator by moving a 1.5 VSWR load through all phases. Referring to a Smith chart, it is seen that the normalized susceptance presented to an oscillator by such loading varies between ± 0.42. Therefore,

$$\frac{d\bar{B}_{OSC}}{d\omega} \approx \frac{\Delta\bar{B}_{OSC}}{\Delta\omega} = \frac{.84}{2\pi L} \, . \tag{7}$$

The parameter L in practice is easier to measure than the oscillator Q.

Using Equations (6) and (7) the stabilization factor can be written as

$$S = 1 + \frac{2\bar{C}_c / (\bar{G}_S \bar{G}_c + 1)^2}{.84 / 2\pi L} \, .$$

Substituting measurable quantities,

$$S = 1 + \frac{2.4 Q_o L}{f_r \beta_1 [\bar{G}_S (\frac{1+\beta_2}{\beta_1}) + 1]^2} \, , \tag{8}$$

where $f_r = \omega_r / 2\pi$.

This result is similar to that obtained by Ashley and Searles [3] but includes the degradation of stabilization caused by G_S.

Graphically, a change in the free running frequency corresponds to a shift in the frequency axis intercept of

the oscillator susceptance curve in Figure 5b. The resulting frequency shift induced in the stabilized system corresponds to the intersection of the oscillator and load susceptance curves ($B_L + B_{OSC} = 0$).

In practice, the unperturbed free running frequency, ω_0, may differ either intentionally or unintentionally from ω_r. Referring again to Figure 5b it is seen that there exists a limitation on the frequency error, $|\omega_0 - \omega_r|$, if a single intersection of the load and (negative) oscillator susceptance curves is to be maintained; that is, if a single mode of oscillation is to be guaranteed. Specifically, the allowable frequency error, $\Delta\omega_E$, corresponds to the value of $|\omega_0 - \omega_r|$ for which the oscillator and load susceptance curves become tangent at $\omega = \omega_r \pm \Delta\omega_A$.

Practical systems satisfy the condition,

$$\bar{G}_S^2 \ll 1.$$

Then, as shown in Appendix 1, the normalized frequency shift, $\Delta\omega_B/\omega_r$ at which $\bar{B}_L = 0$ is essentially independent of $\bar{G}_S$ and is given by,

$$\frac{\Delta\omega_B}{\omega_r} = \pm \, (2\pi N \sqrt{\bar{C}_c/\bar{L}_c})^{-1/2} \tag{9}$$

where N, an odd integer, is the electrical length of the intermediate transmission line in units of $\lambda_r/2$.

Numerical calculations show this approximation to be accurate within 0.5% for the example system. Since $\left|\dfrac{d\bar{B}_L}{d\omega}\right|$ is monotonically decreasing in $|\omega-\omega_r|$ for $|\omega-\omega_r| > |\Delta\omega_\rho|$ the allowable frequency error is maximized for the case $\Delta\omega_A = \Delta\omega_B$; that is, when the point of tangency of $-\bar{B}_{OSC}$ and $\bar{B}_L$ falls on the zero crossing of $\bar{B}_L$. The value of $\bar{G}_S$ required to realize the condition,

$$\frac{d\bar{B}_L}{d\omega}\bigg|_{\omega_r \pm \Delta\omega_B} = - \frac{d\bar{B}_{OSC}}{d\omega} \tag{10}$$

is presented in Section II.

The maximum allowable frequency error is then,

$$\frac{\Delta\omega_{E(max)}}{\omega_r} = \frac{\Delta\omega_B}{\omega_r} = \left(2\pi N\sqrt{C_c/L_c}\right)^{-1/2}. \tag{11}$$

The corresponding frequency shift in the stabilized oscillator, or the tuning range,

$$\frac{\Delta\omega_{T(max)}}{\omega_r} = \frac{1}{S}\left(2\pi N\sqrt{C_c/L_c}\right)^{-1/2}. \tag{12}$$

Since $\Delta\omega_{E(max)}$ and $\Delta\omega_{T(max)}$ vary with $N^{-1/2}$, short line length is generally desirable.

Equations (11) and (12) differ from those obtained by Shelton [4], who implicitly assumed a relatively low value of S.

Substituting measurable quantities in Equations (11) and (12),

$$\frac{\Delta\omega_{E(max)}}{\omega_r} = (2N\pi Q_0/\beta_1)^{-1/2} \tag{13}$$

and

$$\frac{\Delta\omega_{T(max)}}{\omega_r} = \frac{1}{S}(2N\pi Q_0/\beta_1)^{-1/2} . \tag{14}$$

It is important to note that these expressions are applicable only when the condition of Equation (10) is satisfied. Otherwise some smaller value of $\Delta\omega_E$ will be exhibited, as in the case in Figure 5b.

I-3. SUMMARY OF RESULTS

Using the equivalent circuit of Figure 4 and reasonable approximations concerning the changing electrical length of the intermediate transmission line (cf. Appendix 1), the following information has been obtained.

The stabilization factor, or the reduction in small frequency perturbations which can be realized,

$$S = 1 + \frac{2.4 Q_0 L}{f_r \beta_1 [\bar{G}_S(\frac{1+\beta_2}{\beta_1})+1]^2} .$$

The maximum allowable frequency error,

$$\frac{\Delta \omega_{E(max)}}{\omega_r} = (2N\pi Q_0 / \beta_1)^{-1/2} .$$

The tuning range or the maximum value of $|\omega - \omega_r|$ over which the system may be operated,

$$\frac{\Delta \omega_{T(max)}}{\omega_r} = \frac{1}{S} (2N\pi Q_0 / \beta_1)^{-1/2} .$$

$$\frac{\Delta \omega_{E(max)}}{\omega_r} = (2N\pi Q_0 / \beta_1)^{-1/2} .$$

II. DESIGN

II-1. MINIMUM SHUNT CONDUCTANCE

In general, the load susceptance presented to the oscillator is dependent upon changes with frequency in both the susceptance of the stabilizing cavity and the admittance transformation effected by the intermediate transmission line. For small deviations from ω_r, the latter effect is negligible. Conversely, from the definition of the detuned short position, for frequencies many half-bandwidths of the stabilizing cavity removed from ω_r, the load admittance referred to plane A-A becomes essentially that exhibited by the circuit shown schematically in Figure 6, where the stabilizing cavity has been replaced by a short circuit at plane B-B. In Figure 7, the exact susceptance function, $\bar{B}_L$, of the example system, cf. Section I., is plotted along with the corresponding susceptance function, $\bar{B}_{L(2)}$, of the simplified circuit of Figure 6, showing excellent agreement far from resonance.

The admittance locus of the stabilization system is also presented using Smith chart coordinates in Figure 8, with selected points marked for comparison with Figure 7.

A single mode of oscillation is guaranteed when the oscillator and load susceptances add to zero at only one frequency. In Figure 7, it is seen that for all $\omega < \omega_r$, $\bar{B}_{L(2)}$ is greater (more positive) than $\bar{B}_L$; the opposite situ-

-16-

ation being true for $\omega > \omega_r$. Further, the absolute value of the slope $\frac{d\bar{B}_{L(2)}}{d\omega/\omega_r}$ is decreasing in $|\omega-\omega_r|$ over the frequency range of interest.

Hence, for the case $\omega_0 = \omega_r$, suppression of extraneous modes of oscillation is guaranteed when the condition,

$$\frac{d\bar{B}_{OSC}}{d\omega/\omega_r} \geq \left| \frac{d\bar{B}_{L(2)}}{d\omega/\omega_r} \right| \tag{15}$$

is satisfied at $\omega = \omega_r$.

This result requires only the restriction that the oscillator susceptance curve be more nearly linear than that of the simplified equivalent circuit over the frequency range under consideration.

As shown in Appendix 2, the slope of the susceptance curve associated with the simplified circuit at ω_r,

$$\frac{d\bar{B}_{L(2)}}{d\omega/\omega_r}\bigg|_{\omega_r} = \frac{N\pi}{2}\left(1 - \frac{2}{\bar{G}_S^2}\right) . \tag{16}$$

The minimum value of normalized shunt conductance required to guarantee mode suppression, $\bar{G}_{S(min)}$, can be defined by applying to Equation (16) the condition of (15) yielding,

$$\bar{G}_{S(min)} = \left[\frac{2}{\dfrac{d\bar{B}_{OSC}}{d\omega/\omega_r}\dfrac{2}{N\pi} + 1} \right]^{1/2} . \tag{17}$$

-17-

Or, in terms of measurable quantities

$$\bar{G}_{S(min)} = \left[\frac{2}{\frac{1.68 f_r}{N \pi L} + 1} \right]^{1/2} . \tag{18}$$

Most practical systems satisfy the condition,

$$\frac{d\bar{B}_{OSC}}{d\omega/\omega_r} \frac{2}{N\pi} \gg 1 \tag{19}$$

then, Equation (17) becomes

$$\bar{G}_{S(min)} \approx \left[\frac{N\pi}{\frac{d\bar{B}_{OSC}}{d\omega/\omega_r}} \right]^{1/2} = \left[\frac{N\pi L}{.84 f_r} \right]^{1/2} . \tag{20}$$

For the case $N = 1$, and values of $\frac{d\bar{B}_{OSC}}{d\omega/\omega_r} > 50$ (corresponding to oscillator external Q in excess of 25) this approximation yields at most 2% error.

Hence, the minimum suppression conductance can be specified as a function of $\frac{d\bar{B}_{OSC}}{d\omega/\omega_r}$ and line length only, independent of the parameters of the stabilizing cavity.

Strictly, the often used criterion of having the detuned admittance locus of the stabilizing system pass through a "sink" on the oscillator Rieke diagram is neither a necessary nor a sufficient condition for mode suppression. It guarantees only that oscillation can not occur in a limited frequency range near $|\omega - \omega_r| \approx \Delta\omega_B$ where $\bar{G}_L \approx 1/\bar{G}_S$. In addition, this criterion can, depending upon oscillator parameters, lead to an excessively large choice of $\bar{G}_S$.

In Figure 9, $\bar{G}_{S(min)}$ is plotted as a function of line length and $\frac{d\bar{B}_{OSC}}{d\omega/\omega_r}$. For most practical systems,

$$2000 > \frac{d\bar{B}_{OSC}}{d\omega/\omega_r} > 50$$

or,

$$1000 > Q_{EXT} > 25.$$

For the case $N = 1$, such systems require values of $\bar{G}_{S(min)}$ lying between 0.04 and 0.25.

II-2. OPTIMUM SHUNT CONDUCTANCE

In order to maximize the allowable difference between the free running oscillator frequency and the stabilizing cavity resonant frequency, the slopes of the oscillator and load susceptance curves must exhibit the same absolute value at $\omega = \omega_r \pm \Delta\omega_B$; cf. Figure 5b. As shown in Appendix III, Equation (A-11), the rate of change of $\bar{B}_L$ with respect to frequency at these points,

$$\frac{d\bar{B}_L}{d\omega/\omega_r}\bigg|_{\omega_r \pm \Delta\omega_B} \approx \frac{N\pi}{2}\left[1 - \frac{4}{\bar{G}_S^2}\right], \tag{21}$$

is essentially independent of the stabilizing cavity parameters, this result being accurate for the example system to within 2%.

Applying the condition of Equation (10) to the stabilization network yields,

$$\frac{N\pi}{2}\left[1 - \frac{4}{\bar{G}_{S(OPT)}}\right] = -\frac{d\bar{B}_{OSC}}{d\omega/\omega_r} ,$$

where $\bar{G}_{S(OPT)}$ is the normalized value of shunt conductance required to maximize allowable frequency error. Rearranging,

$$\bar{G}_{S(OPT)} = \left[\frac{4}{\frac{d\bar{B}_{OSC}}{d\omega/\omega_r}\frac{2}{N\pi} + 1}\right]^{1/2} , \quad (22)$$

or substituting measurable quantities,

$$\bar{G}_{S(OPT)} = \left[\frac{4}{\frac{1.68f_r}{N\pi L} + 1}\right]^{1/2} . \quad (23)$$

As an illustration, a stabilizing system having parameters $N = 1$ and $\frac{d\bar{B}_{OSC}}{d\omega/\omega_r} = 155$ requires $\bar{G}_{S(OPT)} = 0.2$. In Figure 10 the load susceptance function of Figure 5b is repeated along with the negative of the susceptance function associated with such an oscillator. These curves exhibit tangency, to within graphical accuracy at $\omega = \omega_r \pm \Delta\omega_B$ the maximum allowable frequency error.

From Equations (16) and (21) the slope $\frac{d\bar{B}_{OSC}}{d\omega/\omega_r}\bigg|_{\omega_r \pm \Delta\omega_B}$, for stabilization systems satisfying inequality (19), is very nearly twice that exhibited by the simplified circuit of Figure 6 at $\omega = \omega_r$. For such systems, the optimum con-

ductance can therefore be determined by substituting $2 \frac{d\bar{B}_{OSC}}{d\omega/\omega_r}$ for $\frac{d\bar{B}_{OSC}}{d\omega/\omega_r}$ in Equation (19). Equivalently,

$$\bar{G}_{S(OPT)} \approx \sqrt{2} \; \bar{G}_{S(min)}. \tag{24}$$

In practice, the value of shunt conductance chosen should depend on the oscillator characteristics and intended application. For example, an oscillator subject to large amounts of frequency drift with temperature would require $\bar{G}_{S(OPT)}$ in order to minimize the likelihood of multiple resonances.

Shunt conductance values in excess of $\bar{G}_{S(OPT)}$ should be avoided since both S and $\Delta\omega_E$ are decreasing functions of shunt conductance for $\bar{G}_S > \bar{G}_{S(OPT)}$.

II-3. OPTIMUM LOADING

Mullen [5] shows that the effects of amplitude modulation perturbations are minimized when an oscillator is loaded for maximum power output. Since both A.M. and F.M. noise components degrade signal quality, minimization of A.M. noise is a reasonable design objective in stabilization systems.

Optimum loading (source resistance = load resistance) is most easily achieved by matching both the oscillator driving point resistance, and that exhibited by the stabilization system at resonance, to the intermediate transmission line.

At $\omega = \omega_r$ the normalized load conductance is from
Equation (5a),

$$\bar{G}_L(\text{resonance}) = \frac{1}{\bar{G}_S + 1/\bar{G}_c},$$

or, in terms of the coupling coefficients of the stabilizing
cavity,

$$\bar{G}_L(\text{resonance}) = \frac{1}{\bar{G}_S + \frac{\beta_1}{1 + \beta_2}}. \tag{25}$$

Rearranging Equation (25), the relationship between β_1 and β_2
required to achieve matched loading,

$$\frac{\beta_1}{1 + \beta_2} = (1 - \bar{G}_S). \tag{26}$$

When Equation (26) is satisfied, β_2 can be eliminated
from the stabilization Equation (8) yielding,

$$S = 1 + \frac{2.4 Q_o L}{f_r \beta_1 \left(\frac{1}{1 - \bar{G}_S}\right)^2}$$

from which the degradation of stabilization factor caused by
G_S is apparent.

II-4. INSERTION LOSS

The insertion loss, T_L, is defined as the ratio of the
power absorbed by the useful load of the stabilization sys-
tem, P_L, to the power delivered by the oscillator to a matched

load, P_0.

From the equivalent circuits of Figures 3, 4, and 5, the circuit efficiency of the stabilizing system,

$$\frac{P_L}{P_0'} = \frac{\beta_2}{1+\beta_2} \frac{(\frac{\beta_1}{1+\beta_2})}{\bar{G}_S + (\frac{\beta_1}{1+\beta_2})}$$

where P_0' is the power output of the oscillator loaded by the stabilizing system.

Applying the condition of Equation (26), this result becomes equal to the insertion loss and reduces to,

$$T_L = \frac{P_L}{P_0} = \frac{\beta_2}{1+\beta_2} (1-\bar{G}_S). \tag{27}$$

In Figure 11, where it is assumed that Equation (26) is satisfied, T_L is plotted as a function of β_2 with shunt conductance as a parameter.

Increased power output is realized at the expense of reduced stabilization factor since S varies as $1/\beta_1$. In practice, tolerable insertion loss can be specified as a design objective, from which the required coupling coefficients can be computed.

II-5. DESIGN PROCEDURE

The following steps can be used in specifying system parameters.

(1) From measurements of the oscillator's pulling factor and length of the intermediate transmission line, $\bar{G}_S$ is computed using Equations (18) or (23).

(2) The tolerable insertion loss can be specified, from which the output coupling coefficient β_2 is determined using Equation (27).

(3) Using Equation (26) the input coupling coefficient β_1 required for matched loading is computed.

(4) The stabilization factor and, where applicable, maximum allowable frequency error and tuning range are available from the major results of Section I (cf. p. 14).

III. EXPERIMENTATION

III-1. SYSTEM CONSTRUCTION

Experimental investigation was performed using an IMPATT diode oscillator operating at 9.28 GHz. The oscillator is coupled through a $3\lambda_r/2$ section of x-band waveguide to a high Q circular-cylindrical cavity operating in the TE_{013} mode. One endplate of the stabilizing cavity is electrically isolated from the cylinder wall in order to decouple the TM_{113} mode which satisfies the same boundary conditions. The intermediate waveguide is composed of shims of varying thickness which allow construction of the exact line length required.

In order to realize the stabilization network of Figure 1, accurate determination of the electrical line length, the suppression conductance, and the locations of the detuned short planes of the oscillator and stabilizing cavities are required. An H.P. 8410A network analysis was used in these measurements to display both magnitude and phase of reflection coefficient, referred to a moveable reference plane.

The following procedure was found to be efficient in system construction.

(1) The oscillator is matched to the intermediate transmission line (maximum power into a matched load) and its pulling factor determined using the microwave network shown schematically in

Figure 12. The moveable short is then adjusted to produce zero frequency pulling. The reference position near the mounting plane, from which this admittance is purely real, is then located and corresponds to the detuned short plane of the oscillator cavity.

(2) With the input port of the stabilizing cavity shorted, the output coupling coefficient, β_2, is established. The detuned short position of port 2 is unimportant since the useful load is matched to the transmission line.

(3) The input coupling coefficient, β_1, is set to the required value and its corresponding detuned short position located.

(4) Waveguide shims are added to the stabilizing cavity input port and the suppression conductance, cf. Section III-2., is introduced an odd number of quarter wavelengths from the detuned short plane. The admittance of the stabilizing cavity and suppression conductance, referred to the plane of G_S, is measured and line length adjusted if necessary.

(5) Additional shims are added to locate the oscillator detuned short plane an odd number of quarter wavelengths from the suppression conductance.

The stabilizing system admittance referred to
this plane is measured and line length again
adjusted if required.

(6) The oscillator is coupled to the completed sta-
bilization system and tuned to yield maximum
stabilization factor. This can be accomplished
by applying a modulating signal at a frequency,

$$f_m < Q_o/2f_r,$$

i.e., modulation frequency within the pass band
of the stabilizing cavity. Side band intensities
are observed on a spectrum analyzer, maximum
stabilization corresponding to minimum side band
intensity.

III-2. REALIZATION OF SUPPRESSION CONDUCTANCE

Generally, introduction of an obstacle into a wave-
guide produces both conductive and susceptive components.
In order to accurately introduce the suppression conductance,
it is required that the susceptive component be eliminated
and also that the physical width of the resistive element
(distance along waveguide) be small compared to a wavelength;
thereby, producing a simple conductance rather than a π net-
work.

The above conditions were found to be effectively met by the structure shown in Figure 13. A small piece of 250 ohm/square mica-backed metal resistive card measuring approximately .4" x .1" x .001" is introduced from one of the broad walls of an x-band waveguide shim. In order to provide variable conductance, the depth of penetration is made adjustable. This element introduces a small capacitive susceptance ($\bar{B} \approx 0.05$ for $\bar{G}_S = 0.2$), an effect which is eliminated by inserting thin inductive screws from the narrow walls of the waveguide shim in the same plane as the suppression conductance. The frequency dependence associated with this cancellation is negligible for high Q systems.

III-3. EXPERIMENTAL RESULTS

Measured parameters of the experimental stabilization system and oscillator are: $Q_0 = 21,600$, $\beta_1 = .91$, $\beta_2 = .143$, $L = 22.0$ MHz., $\bar{G}_S = 0.2$ and $\ell = 3$.

The value of shunt conductance used was somewhat larger than $\bar{G}_{S(OPT)}$, due to difficulty in selecting a suitable oscillator and the extensive changes in the stabilization system required to alter the suppression conductance.

Using Equations (8) and (27) the above parameters yield theoretical values of stabilization factor and insertion loss,

$$S = 87.4$$
$$T_L = -9.9 \text{ dB}$$

Measured insertion loss was -10.5 dB, in good agreement with the predicted value.

The stabilization factor was determined by applying a modulating signal, with and without the stabilizing system, and measuring suppression of F.M. side bands. For small frequency deviations, the magnitude of first order side bands is proportional to the modulation index, $\Delta f/f_M$ where Δf is the peak frequency shift induced in the oscillator and f_M is the modulating signal frequency.

Since Δf is reduced by a factor of $1/S$ in the stabilized oscillator, the stabilization factor is simply the ratio of free running to stabilized side band magnitudes, for constant modulating signal. In terms of side band power, P_{SB},

$$\frac{P_{SB(FR)}}{P_{SB(S)}} = S^2$$

Measured data from an H.P. 8551B spectrum analyzer display were as follows:

f_M(KHz)	$\dfrac{P_{SB(FR)}}{P_{SB(S)}}$ (dB)
50	41
75	40
100	38

The theoretical stabilization factor of 87.4 corresponds to a predicted side band power suppression of 38.8 dB. Agreement between experimental and theoretical values is good and is within the measurement accuracy of the spectrum analyzer.

From Equation (14), the maximum tuning range associated with the experimental system,

$$\Delta\omega_{T(max)} = 159 \text{ KHz}.$$

Since the shunt conductance, $\bar{G}_S > \bar{G}_{S(OPT)}$, some lesser tuning range is predicted. Experimentally, oscillations were found to not build up outside a 200 KHz bandwidth centered at approximately $\omega = \omega_r$, i.e.,

$$\Delta\omega_T \approx 100 \text{ KHz}.$$

Once established, however, oscillation was maintained over a frequency range,

$$|\omega - \omega_r| < 400 \text{ KHz}.$$

These results are consistent with the predicted tuning range since the introduction of multiple resonant frequencies need not destroy existing oscillation but can prevent the build-up of oscillations as explained by Rieke [1].

Free running and stabilized noise performance [8] of the
IMPATT oscillator are presented in Figures 14 and 15.
Measured suppression of F.M. noise power varies between
30.0 dB and 39.8 dB, while A.M. data shows good agreement of
noise power for free running (matched load) and stabilized
operations.

APPENDIX 1

DERIVATION OF NORMALIZED FREQUENCY SHIFT
CORRESPONDING TO ZERO CROSSING OF LOAD SUSCEPTANCE

Let $\bar{Y}_L' = \bar{G}_L' + j\bar{B}_L'$ denote the normalized admittance of the stabilizing cavity, load and suppression conductance referred to the plane of G_S. At the zero crossings of the load susceptance, $\bar{B}_L$, referred to plane A-A,

$$\bar{B}_L = \text{Im}(\bar{Y}_L) = \text{Im}\left[\frac{\bar{G}_L' + j(\bar{B}_L' + \tan\beta\ell)}{1 - \bar{B}_L'\tan\beta\ell + j\bar{G}_L'\tan\beta\ell}\right] = 0$$

where β is the wave number. Therefore at $\omega = \omega_r + \Delta\omega_B$ (cf. Figure 5b),

$$\frac{\bar{G}_L'}{1 - \bar{B}_L'\tan\beta\ell} = \frac{\bar{B}_L + \tan\beta\ell}{\bar{G}_L'\tan\beta\ell} \tag{A-1}$$

But,

$$\bar{Y}_L' = \bar{G}_S + \frac{\bar{G}_C + j(\bar{B}_C + \tan\beta\ell)}{(1 - \bar{B}_C\tan\beta\ell) + j(\bar{G}_C\tan\beta\ell)}$$

where $\bar{G}_C$ and $\bar{B}_C$ are the normalized conductance and susceptance respectively of the stabilizing cavity and load referred to plane B-B.

Therefore,

$$\bar{G}_L' \approx G_S + \frac{\bar{G}_C\tan^2\beta\ell + \bar{G}_C}{(\bar{G}_C^2 + \bar{B}_C^2)\tan^2\beta\ell}$$

-32-

and,

$$\bar{B}_L' \approx \frac{-\bar{G}_C^2 \tan\beta\ell + \bar{B}_C + \tan\beta\ell - \bar{B}_C^2 \tan\beta\ell - \bar{B}_C \tan^2\beta\ell}{(\bar{G}_C^2 + \bar{B}_C^2)\tan^2\beta\ell} .$$

Typically $\bar{G}_C \approx 1$. Also, in the neighborhood of $\omega_r + \Delta\omega_B$ (cf. Figure 5b),

$$|\bar{B}_C| \gg 1$$

and

$$|\tan\beta\ell| \gg 1$$

where $\bar{B}_C$ and $\tan\beta\ell$ are of opposite sign.

Hence,

$$\bar{G}_L' \approx \bar{G}_S + \bar{G}_C / \bar{B}_C^2 \approx \bar{G}_S \tag{A-2}$$

and,

$$\bar{B}_L' \approx \frac{-\bar{B}_C^2 \tan\beta\ell - \bar{B}_C \tan^2\beta\ell}{\bar{B}_C^2 \tan^2\beta\ell} = \frac{-\bar{B}_C - \tan\beta\ell}{\bar{B}_C \tan\beta\ell} . \tag{A-3}$$

Since $\bar{B}_L' \ll \tan\beta\ell$ near $\omega_r + \Delta\omega_B$, substituting Equations (A-2) and (A-3) into (A-1) yields,

$$\bar{G}_S^2 \approx 1 - \left(\frac{-\bar{B}_C - \tan\beta\ell}{\bar{B}_C \tan\beta\ell}\right)\tan\beta\ell = 2 + \tan\beta\ell/\bar{B}_C.$$

For practical systems $\bar{G}_S^2 \ll 1$; therefore,

$$\bar{B}_C \approx -\tan\beta\ell/2 \qquad\qquad\qquad\qquad (A-4)$$

at $\omega = \omega_r \pm \Delta\omega_B$.

Employing the Taylor series expansion for $\tan^{-1}$ about $N\pi/2$ where N is an odd integer,

$$\beta\ell \approx \frac{N\pi}{2} + \frac{1}{2\bar{B}_C} = \frac{N\pi}{2} + 1/\left(4\sqrt{C_C/L_C}\ \frac{\Delta\omega_B}{\omega_r}\right)$$

But,

$$\beta\ell = \frac{N\pi}{2}\left(1 + \frac{\Delta\omega_B}{\omega_r}\right)$$

Therefore,

$$\left(\frac{\Delta\omega_B}{\omega_r}\right)^2 = 1/\left(2N\pi\sqrt{C_C/L_C}\right)$$

or

$$\frac{\Delta\omega_B}{\omega_r} = \pm\left(2N\pi\sqrt{C_C/L_C}\right)^{-1/2}. \qquad\qquad (A-5)$$

-34-

APPENDIX 2

DERIVATION OF SLOPE OF SUSCEPTANCE FUNCTION
FOR SIMPLIFIED EQUIVALENT CIRCUIT

The normalized admittance of the simplified circuit of Figure 6, referred to plane A-A,

$$\bar{Y}_{L(2)} = \frac{[\bar{G}_S + j(\tan\beta\ell - 1/\tan\beta\ell)][2 - j(\bar{G}_S\tan\beta\ell)]}{4 + \bar{G}_S^2\tan^2\beta\ell} .$$

The susceptive component,

$$\bar{B}_{L(2)} = \frac{(-\bar{G}_S^2 + 2)\tan\beta\ell - 2/\tan\beta\ell}{4 + \bar{G}_S^2\tan^2\beta\ell} .$$

Evaluating the derivative with respect to $\beta\ell$ at $\beta\ell = N\lambda_r/4$,

$$\frac{d\bar{B}_{L(2)}}{d(\beta\ell)} = \frac{\bar{G}_S^2(2 - \bar{G}_S^2) - (2 - \bar{G}_S^2)(2\bar{G}_S^2)}{\bar{G}_S^4} = 1 - \frac{2}{\bar{G}_S^2}$$

Employing the relationship,

$$\beta\ell = \frac{N\pi}{2}\frac{\omega}{\omega_r}$$

yields

$$\frac{d\bar{B}_{L(2)}}{d\omega/\omega_r} = \frac{N\pi}{2} \left(1 - \frac{2}{\bar{G}_S^2} \right) . \tag{A-6}$$

For the case $\omega_0 = \omega_r$ mode suppression is guaranteed when

$$\frac{d\bar{B}_{OSC}}{d\omega/\omega_r} > \left| \frac{d\bar{B}_{L(2)}}{d\omega/\omega_r} \right|$$

cf. Figure 7. Therefore the minimum suppression conductance,

$$\bar{G}_{S(min)} = \left[\frac{2}{\dfrac{d\bar{B}_{OSC}}{d\omega/\omega_r} \dfrac{2}{N\pi} + 1} \right]^{1/2} \tag{A-7}$$

APPENDIX 3

DERIVATION OF SLOPE OF LOAD SUSCEPTANCE CURVE
AT $\omega = \omega_r \pm \Delta\omega_B$

The susceptance presented to the oscillator,

$$\bar{B}_L = \frac{-\bar{G}_L'^2 \tan\beta\ell + \bar{B}_L' + \tan\beta\ell - \bar{B}_L'^2 \tan\beta\ell - \bar{B}_L' \tan^2\beta\ell}{(1 - \bar{B}_L' \tan\beta\ell)^2 + (\bar{G}_L' \tan\beta\ell)^2} \tag{A-8}$$

where $\bar{Y}_L' = \bar{G}_L' + j\bar{B}_L'$ is defined in Appendix 1. From Equation (A-3),

$$\bar{B}_L' = 1/\tan\beta\ell \quad \text{at} \quad \omega = \omega_r \pm \Delta\omega_B .$$

Then, using Equation (A-2),

$$\frac{d\bar{B}_L}{d(\beta\ell)}\bigg|_{\omega_r \pm \Delta\omega_B} = \frac{[\bar{G}_S^2 \tan\beta\ell][(-1 - \bar{G}_S^2)\tan^2\beta\ell - \frac{d\bar{B}_L'}{d(\beta\ell)}\tan^2] + 2\bar{G}_S^4 \tan^2\beta\ell}{\bar{G}_S^4 \tan^4\beta\ell}$$

$$\approx 1 + \frac{1}{\bar{G}_S^2}\left(-1 - \frac{d\bar{B}_L'}{d(\beta\ell)}\right). \tag{A-9}$$

From Appendix 1,

$$\bar{B}_L' = \frac{-\bar{G}_C^2 \tan\beta\ell + \bar{B}_C + \tan\beta\ell - \bar{B}_C^2 \tan\beta\ell - \bar{B}_C \tan^2\beta\ell}{(1 - \bar{B}_C \tan\beta\ell)^2 + (\bar{G}_C \tan\beta\ell)^2} .$$

Then, using:

$$\tan\beta\ell = -2\bar{B}_C$$

$$|\tan\beta\ell| \gg 1 \qquad\Bigg\} \qquad \text{at } \omega = \omega_r \pm \Delta\omega_B$$

$$\frac{d\bar{B}_C}{d(\beta\ell)} = \frac{\tan^2\beta\ell}{2}$$

$$\frac{d\bar{B}'_L}{d(\beta\ell)}\Bigg|_{\omega_r \pm \Delta\omega_B} \approx \frac{(\tan^4\beta\ell)(3\tan^4\beta\ell)/16}{\tan^8\beta\ell/16} = 3 \ . \tag{A-10}$$

Employing the relationship,

$$\beta\ell = \frac{N\pi}{2}\frac{\omega}{\omega_r}$$

substitution of Equation (A-10) into Equation (A-9) yields,

$$\frac{d\bar{B}_L}{d\omega/\omega_r}\Bigg|_{\omega_r \pm \Delta\omega_B} = \frac{N\pi}{2}\left(1 - \frac{4}{\bar{G}_S}\right) \tag{A-11}$$

Tuning range is maximized under the condition of Equation (10),

$$\frac{d\bar{B}_{OSC}}{d\omega/\omega_r} = \left|\frac{d\bar{B}_L}{d\omega/\omega_r}\right|$$

at $\omega = \omega_r$. The shunt conductance required to achieve this condition,

$$\bar{G}_{S(OPT)} = \left[\frac{4}{\dfrac{d\bar{B}_{OSC}}{d\omega/\omega_r} \dfrac{2}{N\pi} + 1} \right]^{1/2}$$

(A-12)
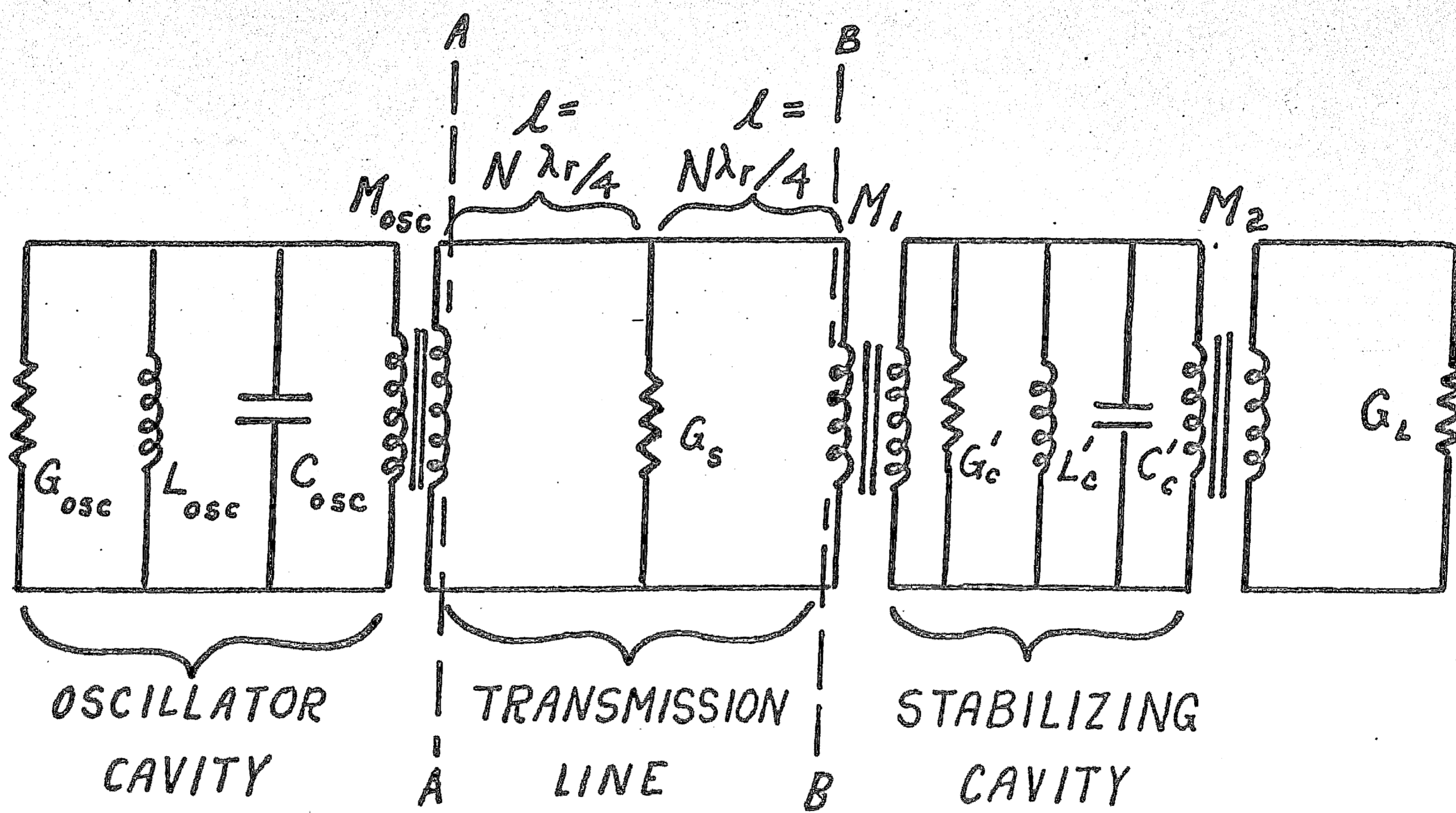
Figure 1 - Stabilization System
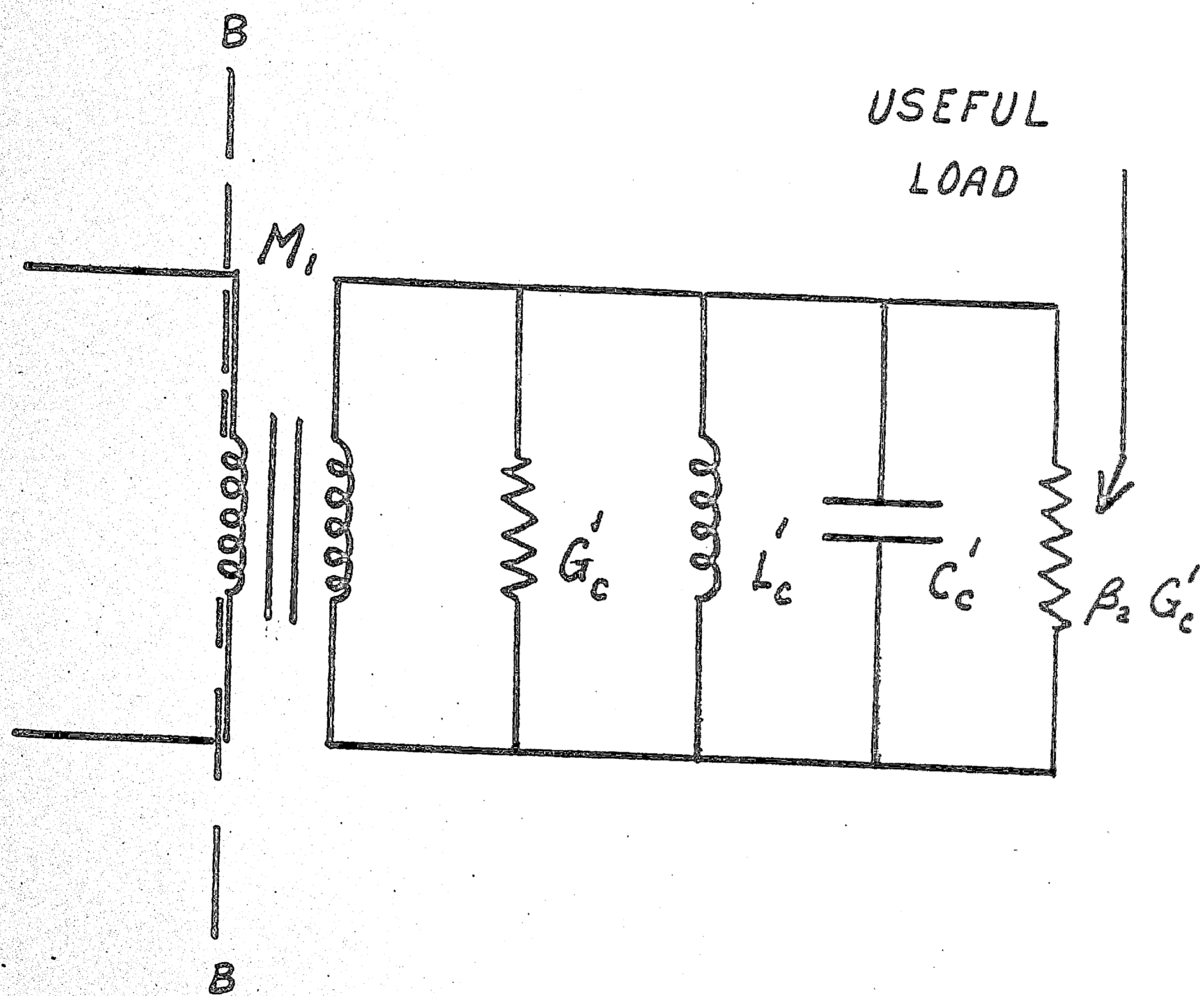
Figure 2 - Load Conductance Lumped with Stabilizing
Cavity Parameters
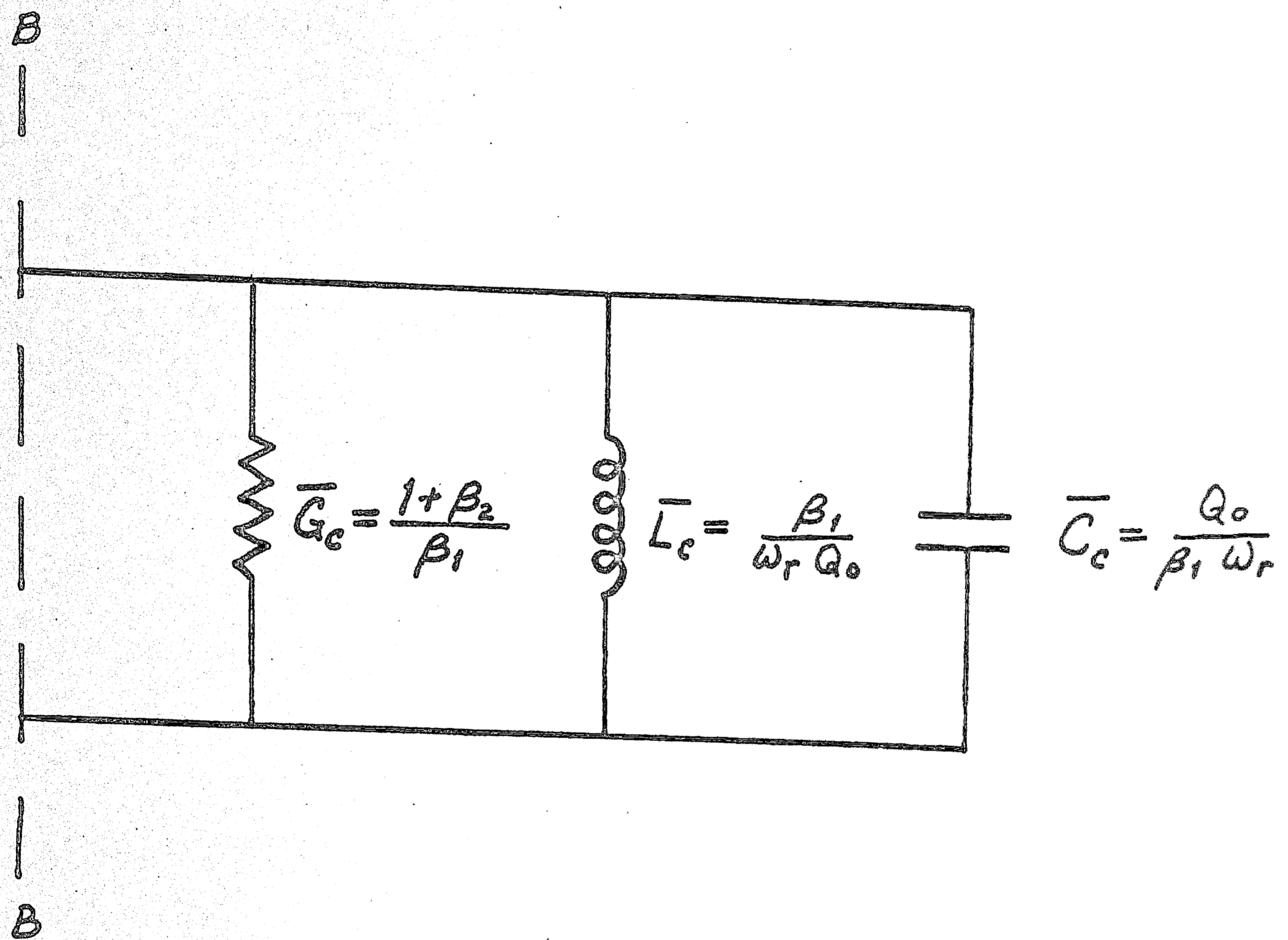
Figure 3 - Equivalent Circuit of Stabilizing Cavity
and Load
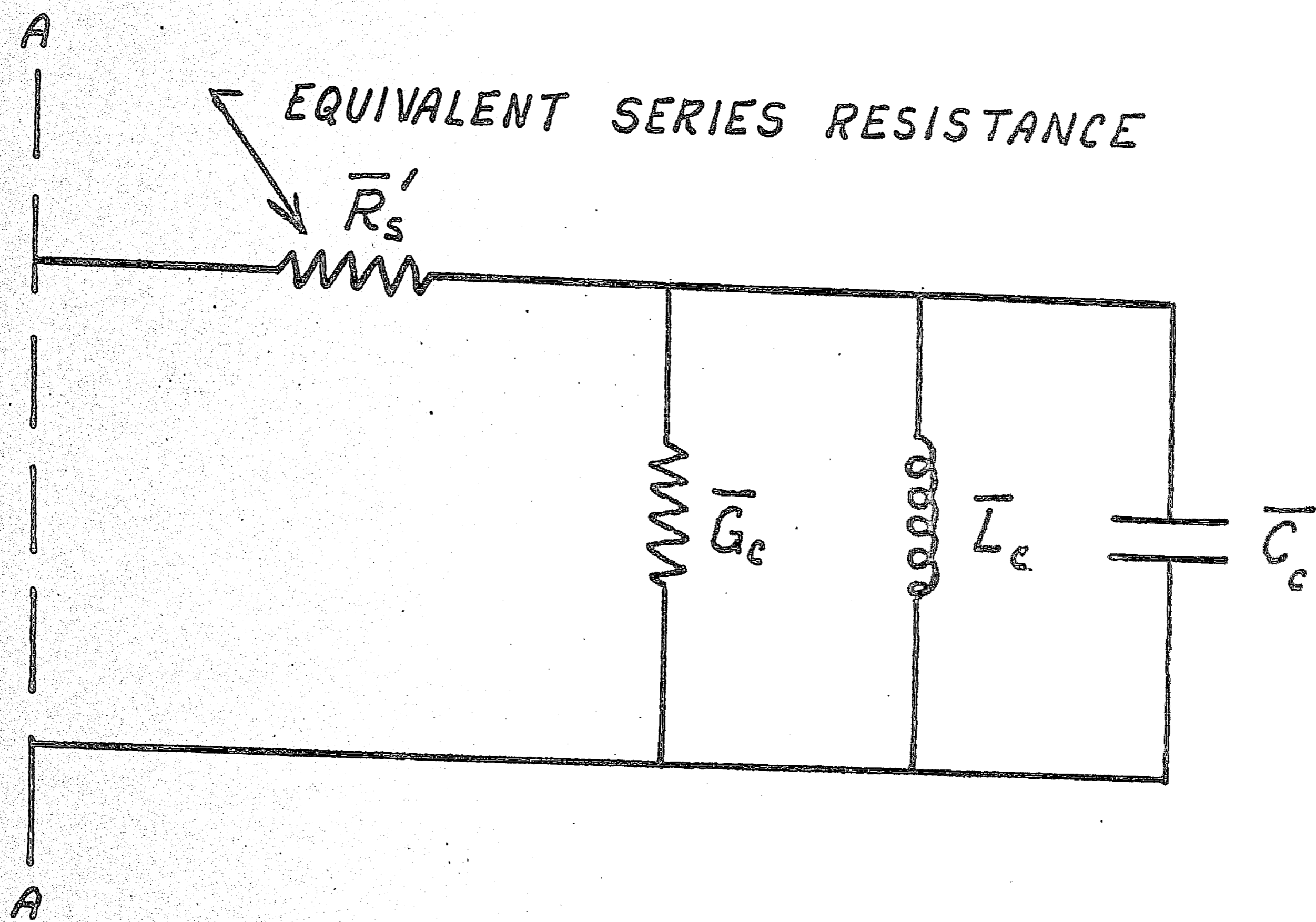
Figure 4 - Equivalent Circuit of Stabilization System
for $\lambda = \lambda_r$
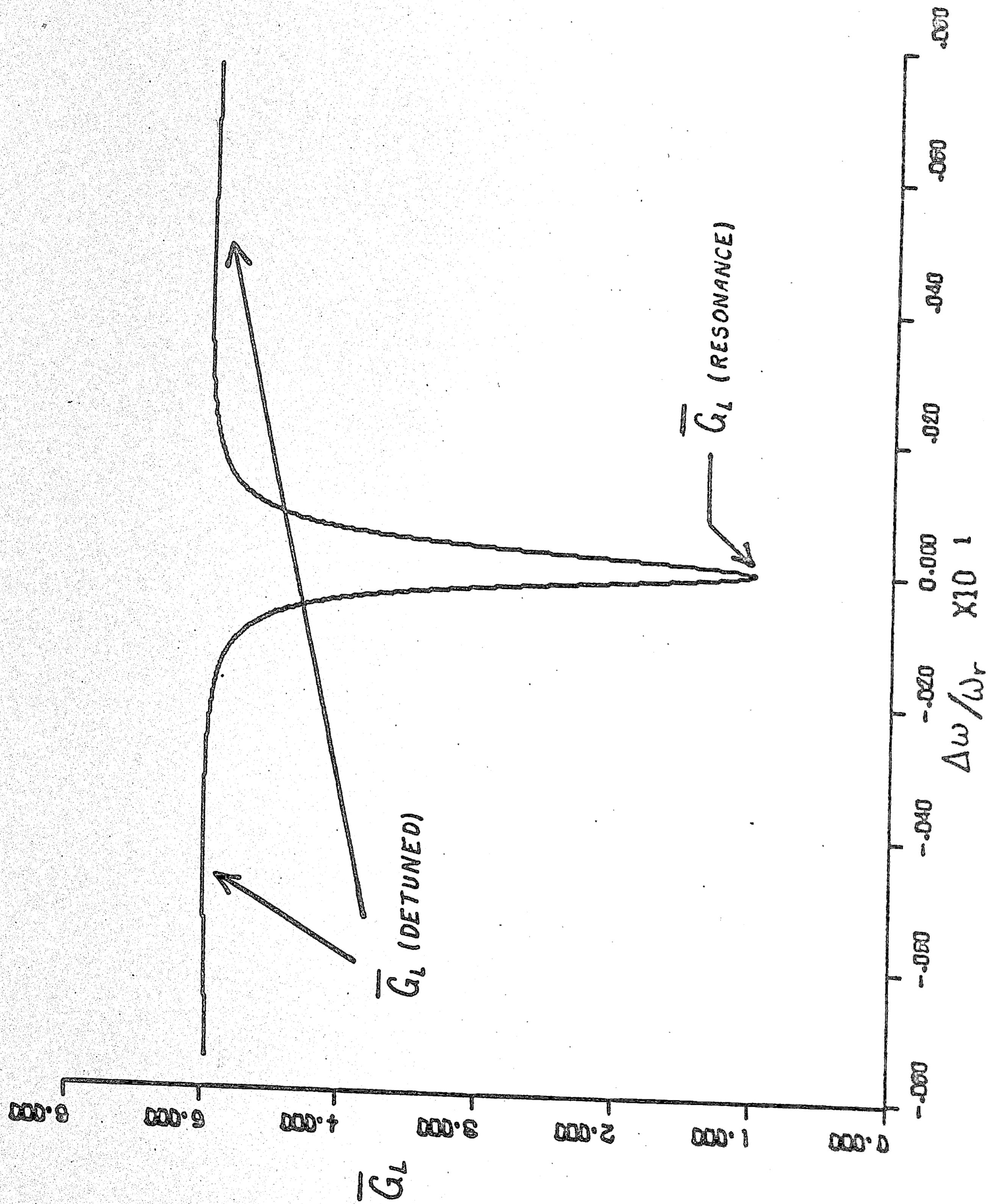
Figure 5a - Conductance Function of Stabilization System
Near Resonance
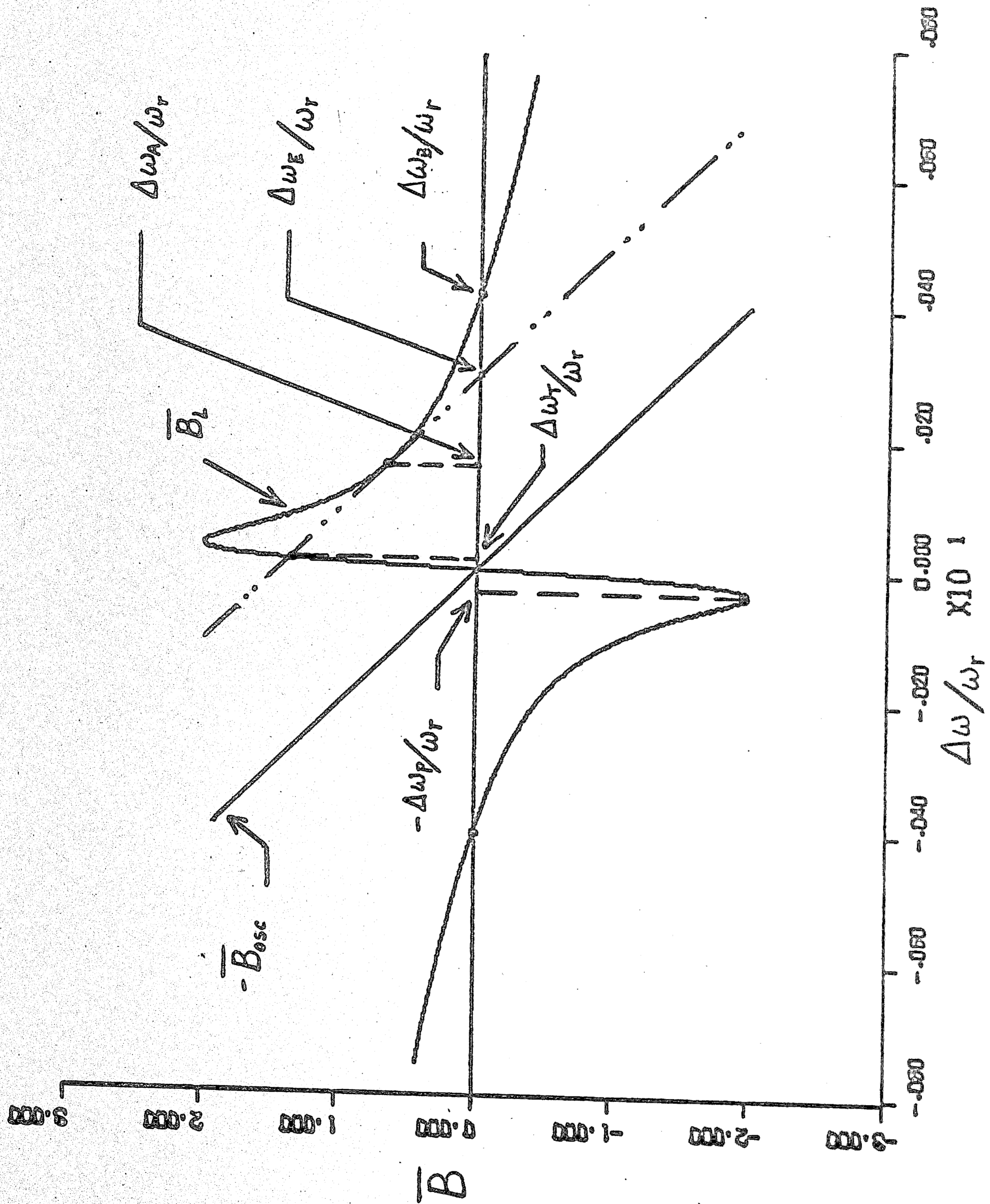
Figure 5b - Susceptance Function of Stabilization System Near Resonance
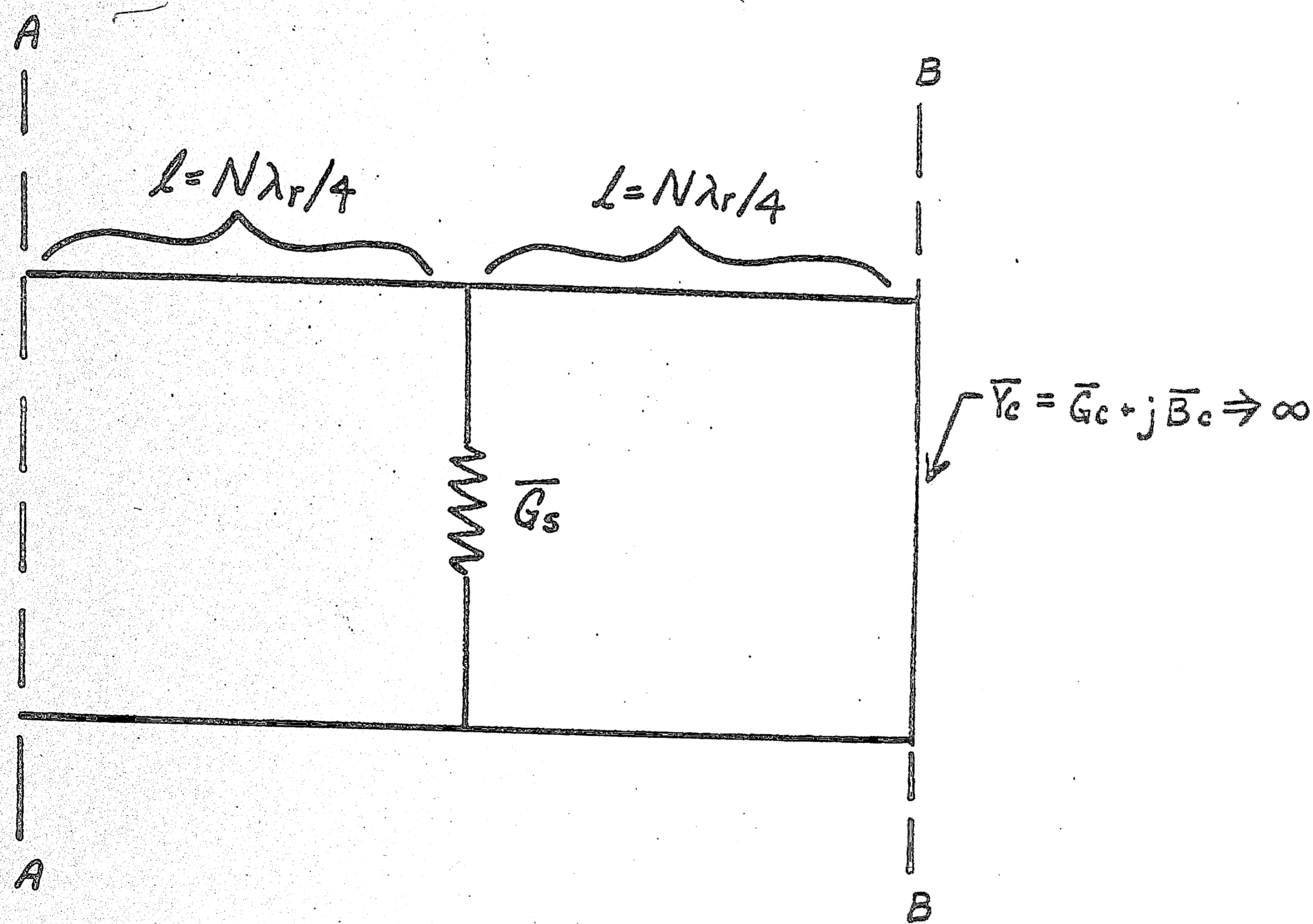
Figure 6 - Simplified Equivalent Circuit Far from Resonance
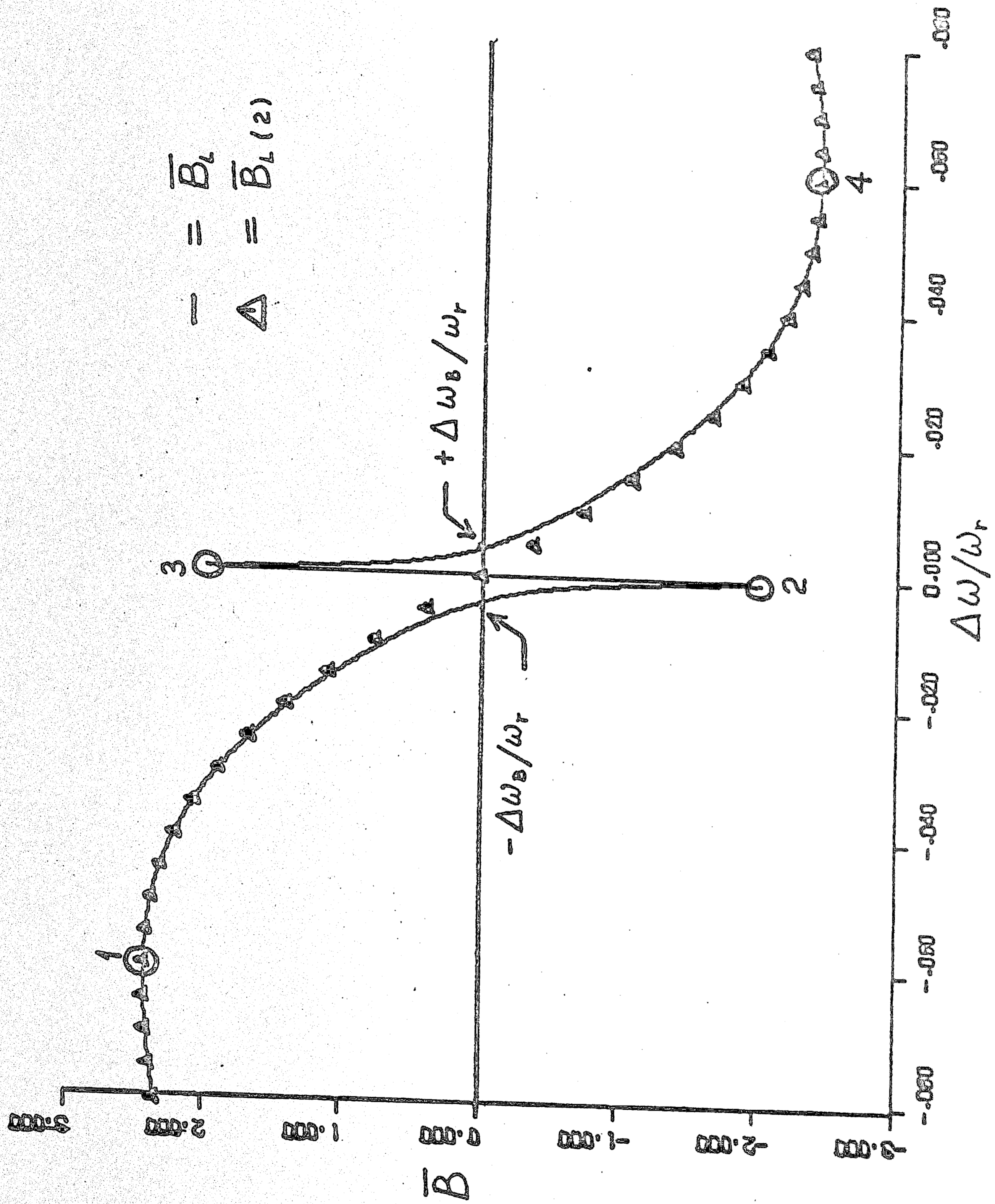
Figure 7 - Susceptance Functions of Stabilization System
and Simplified Equivalent Circuit
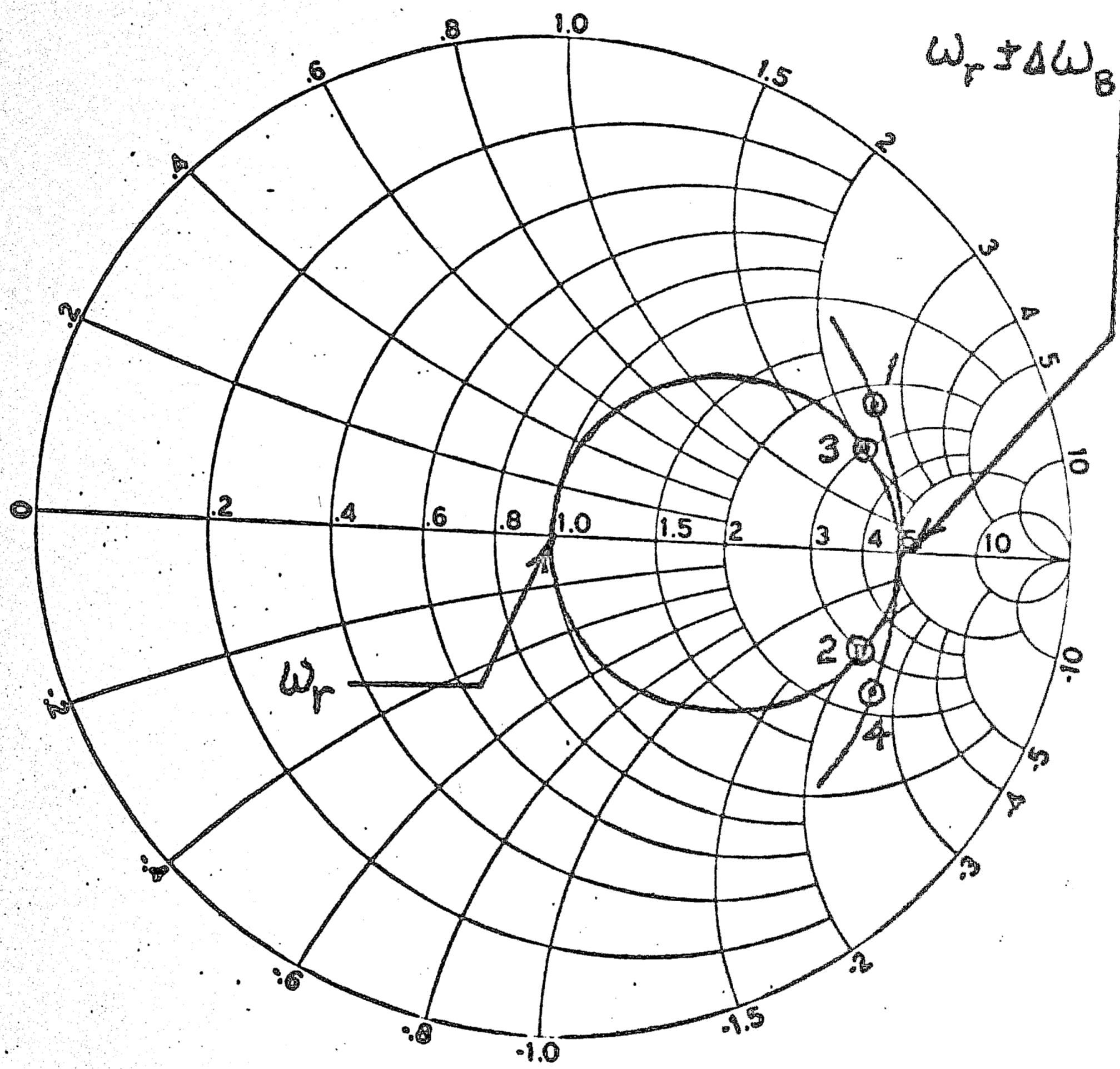
ADMITTANCE COORDINATES

Figure 8 - Admittance Locus of Stabilization System
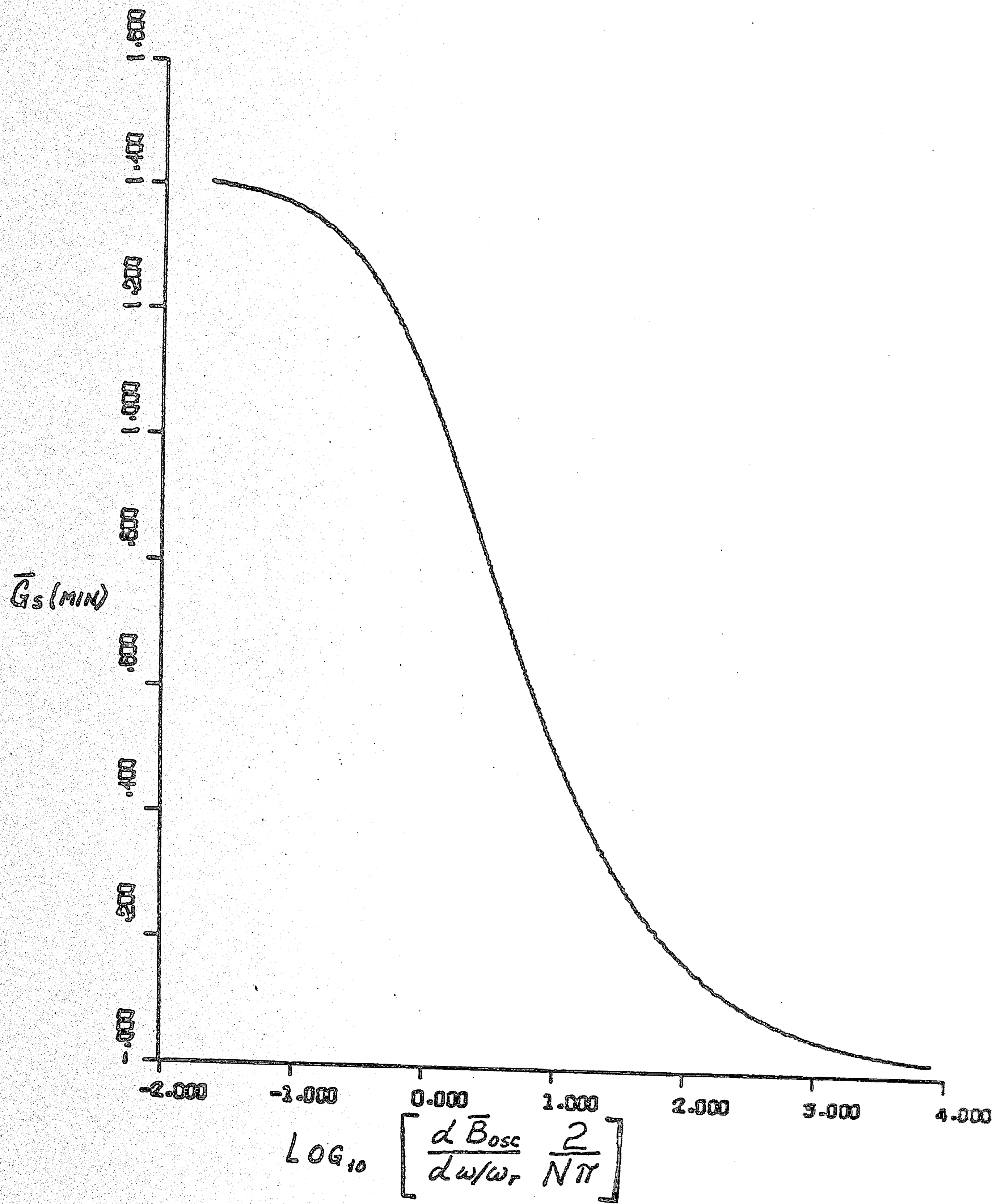
Figure 9 - Minimum Suppression Conductance vs. $\frac{dB_{OSC}}{d\omega/\omega_r}$ and Line Length
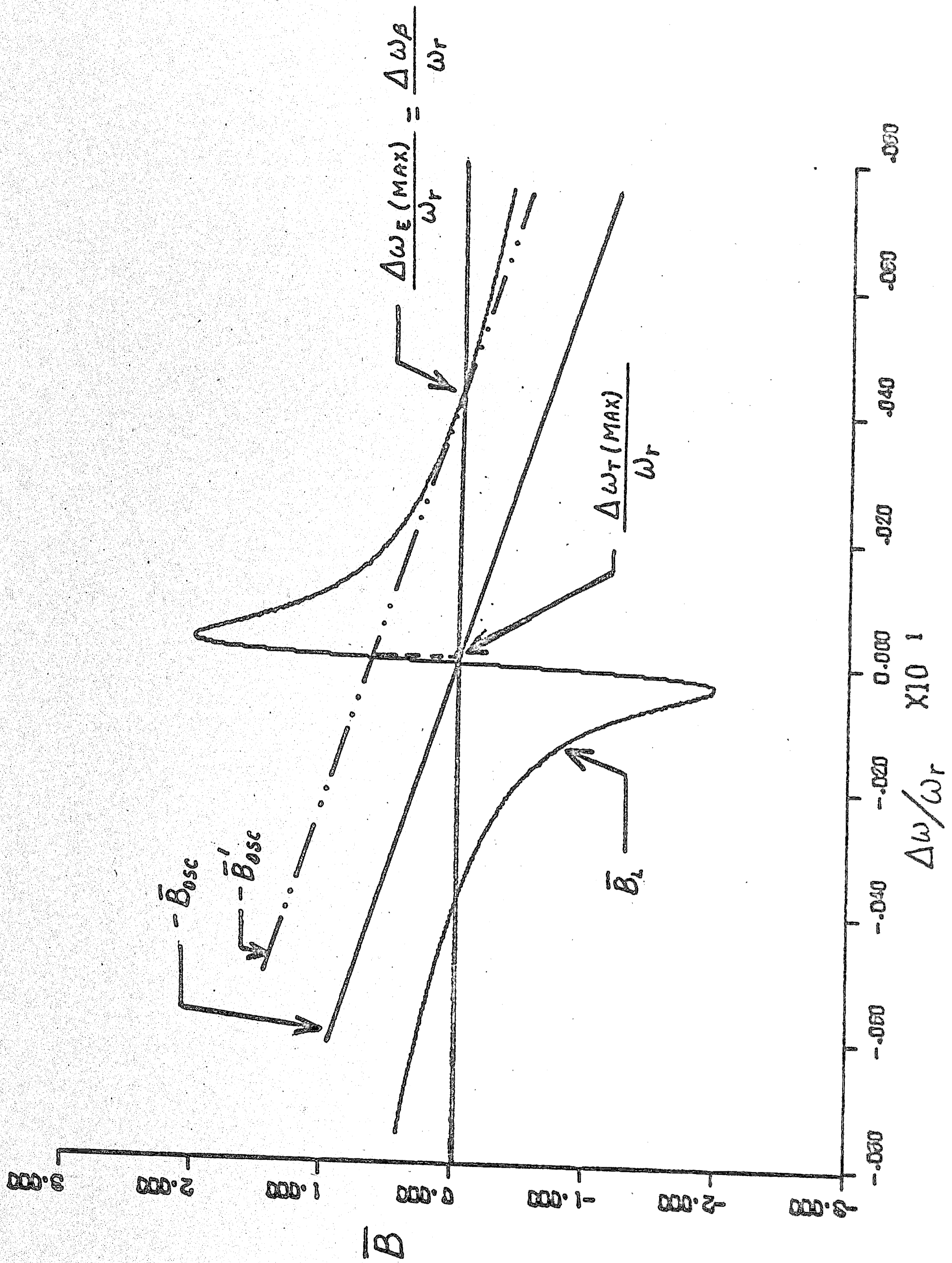
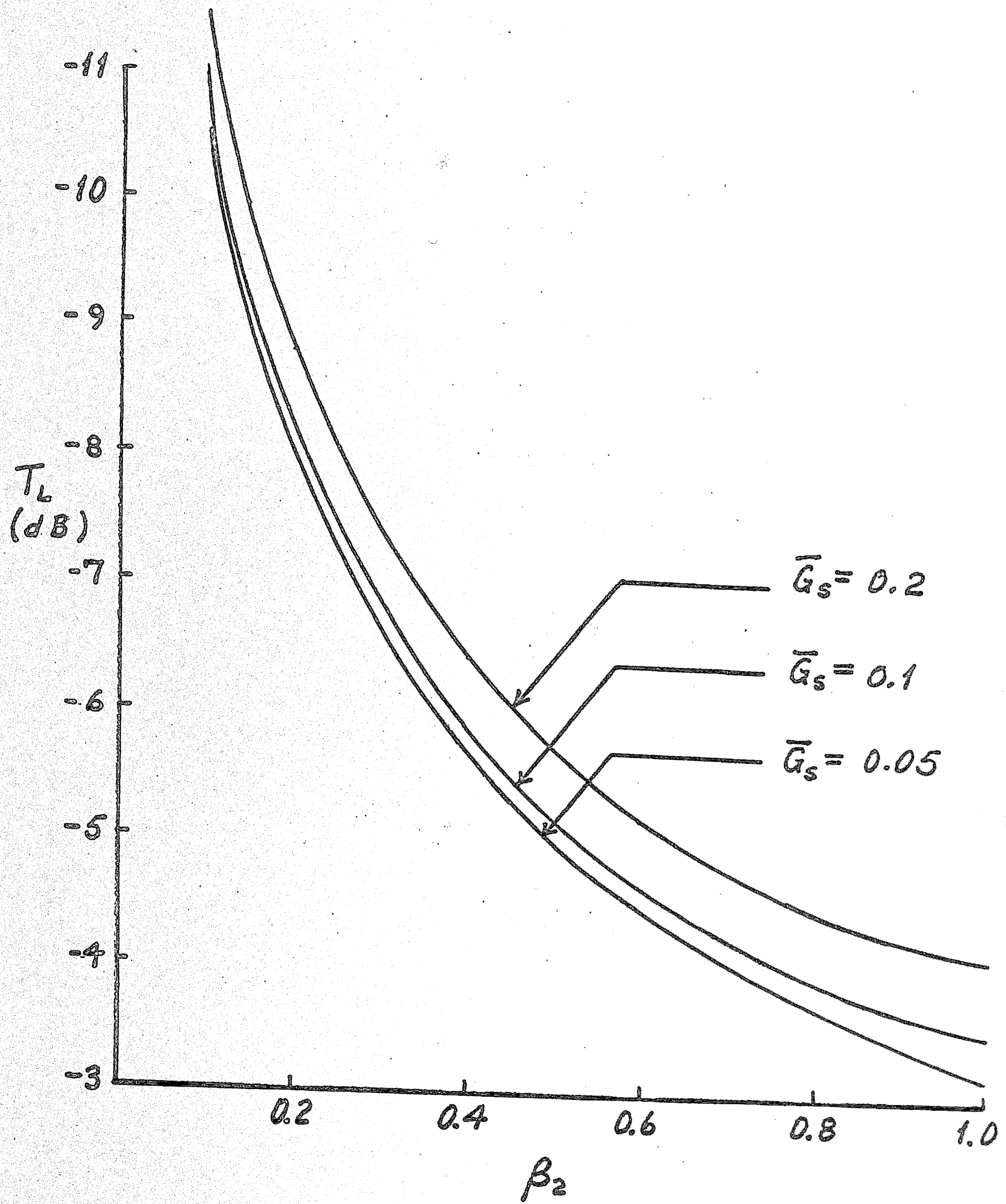Figure 10 - Illustration of Maximized Frequency Error and Tuning Range

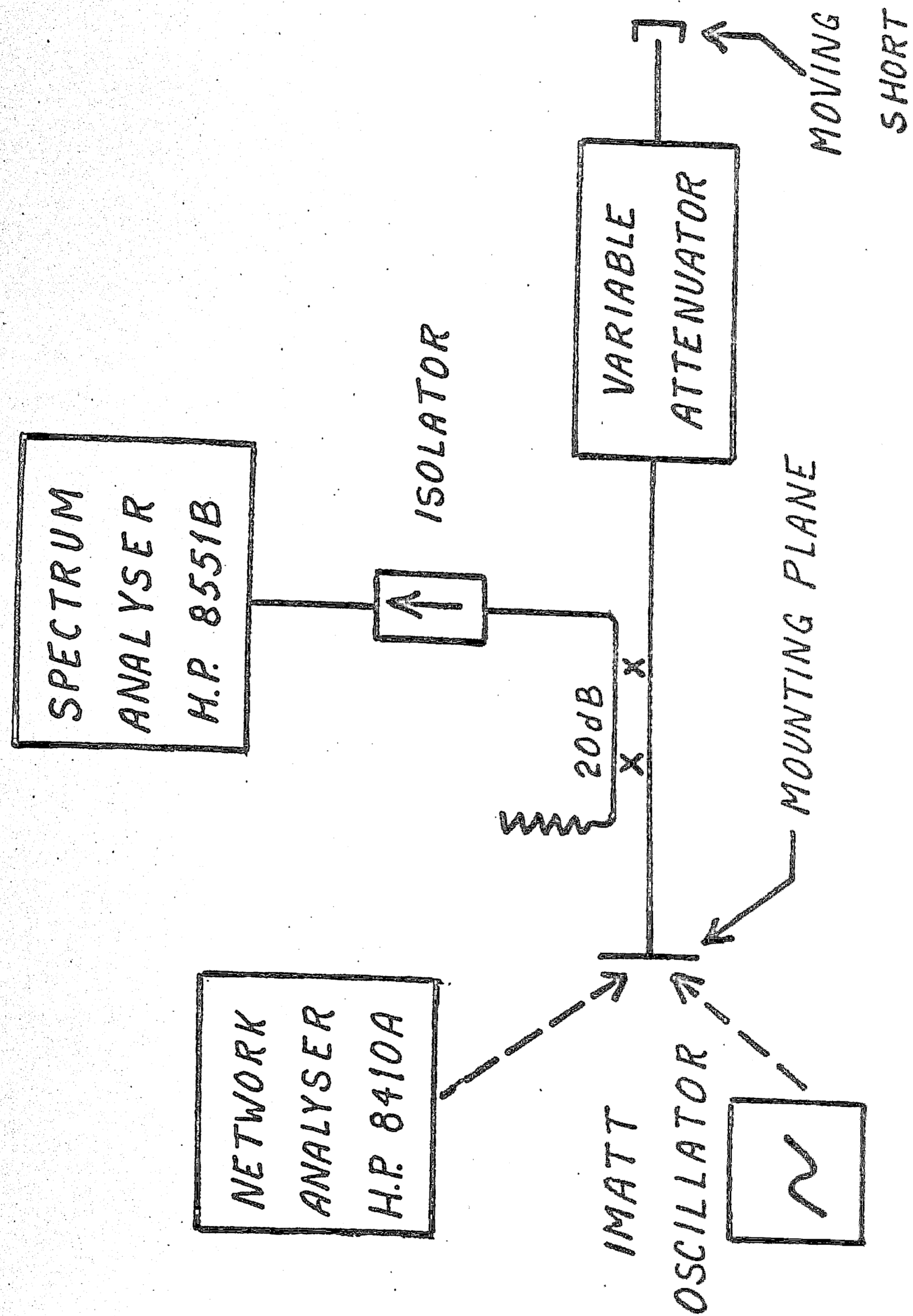Figure 11 - Insertion Loss vs. Output Coupling Coefficient

Figure 12 - Equipment for Measurement of Pulling Factor

PENETRATION
ADJUSTMENT

RESISTIVE
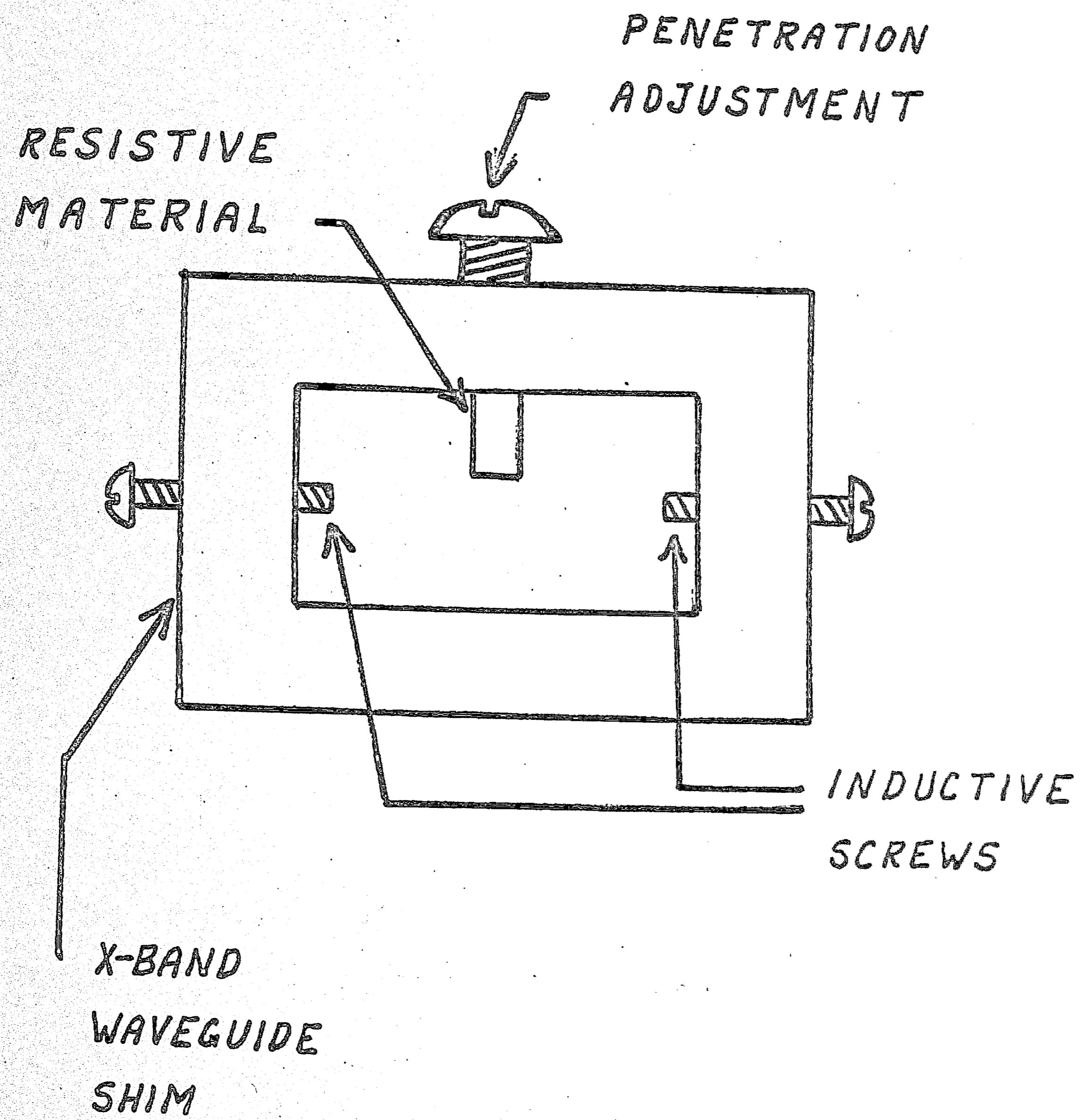MATERIAL

INDUCTIVE
SCREWS

X-BAND
WAVEGUIDE
SHIM
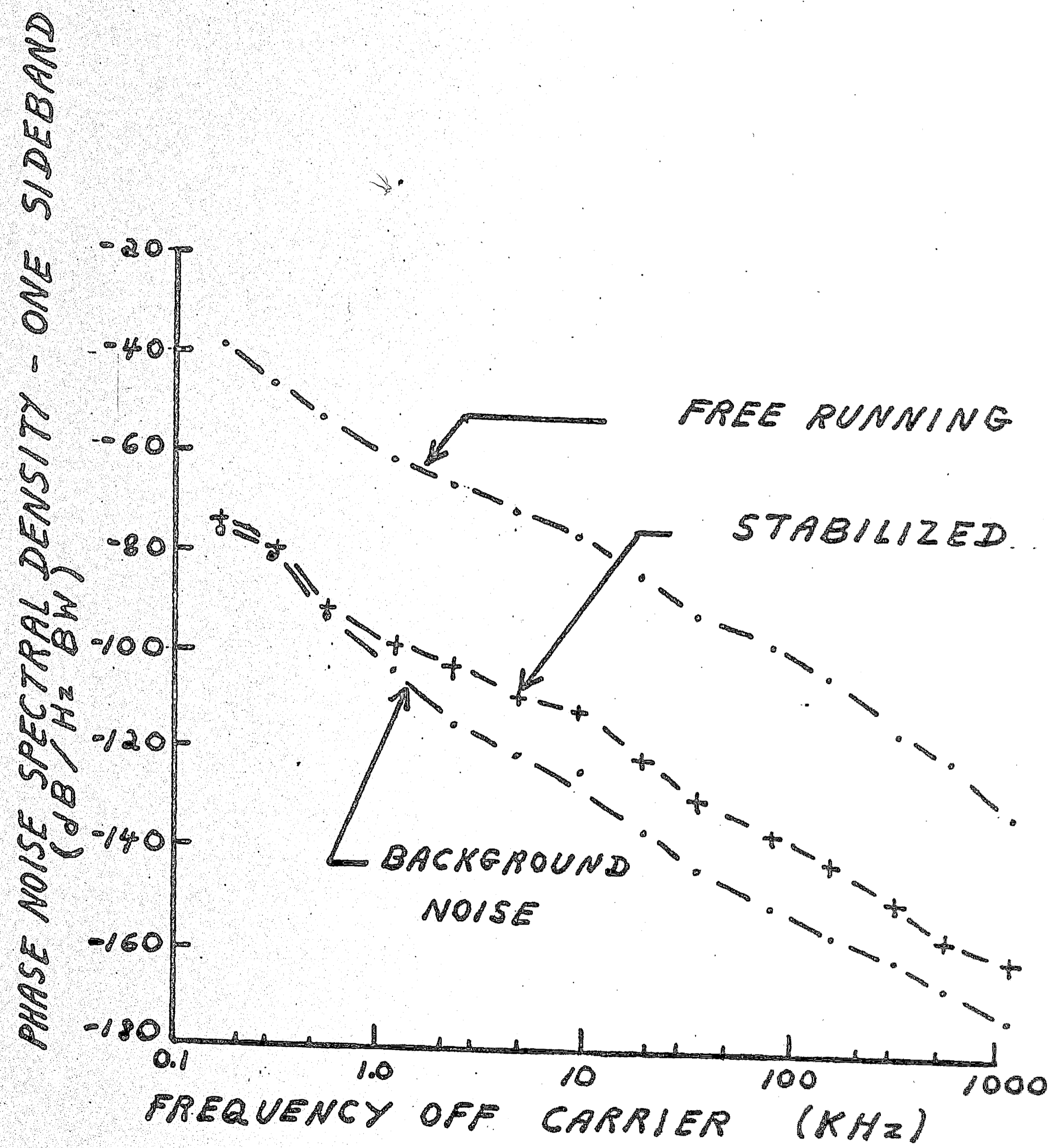
Figure 13 - Suppression Conductance Assembly

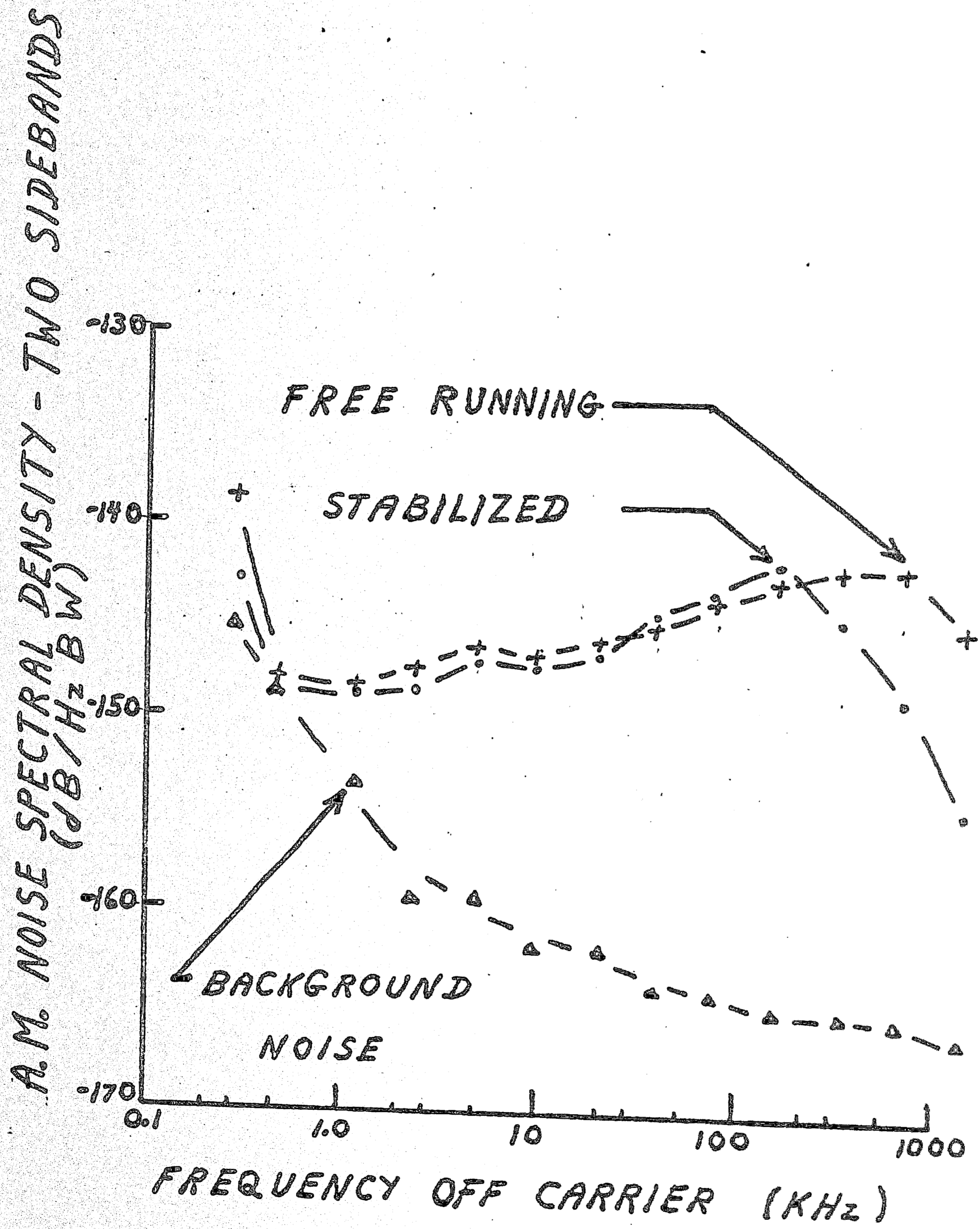Figure 14 - Free Running and Stabilized F.M. Noise
Performance

Figure 15 - Free Running and Stabilized A.M. Noise
Performance

BIBLIOGRAPHY

[1] Rieke, F. F., "Stabilization of Frequency", Chapter 16 of MICROWAVE MAGNETRONS, Vol. 6, Radiation Laboratory Series, McGraw-Hill, 1948.

[2] Ginzton, E. L., MICROWAVE MEASUREMENTS, McGraw-Hill, 1957.

[3] Ashley, J. R. and Searles, C. B., "Microwave Oscillator Noise Reduction by a Transmission Stabilizing Cavity", IEEE Trans. M.T.T., Vol. MTT-16, No. 9, September 1968.

[4] Shelton, E. I., Jr., "Stabilization of Microwave Oscillators", IRE Trans. E.D., Vol. I, No. 4, December 1954.

[5] "Transmission Cavity Stabilization of Klystron Oscillators", Engineering Report, Sperry Electronic Tube Division, 1961.

[6] Goldman, S., FREQUENCY ANALYSIS, MODULATION AND NOISE, McGraw-Hill, 1948.

[7] Montgomery, C. G., Dieke, R. H., and Purcell, E. M., PRINCIPLES OF MICROWAVE CIRCUITS, Vol. 8, Radiation Laboratory Series, McGraw-Hill, 1948.

[8] Ondria, J. G., "A Microwave System for Measurement of AM and FM Noise Spectra", IEEE Trans., M.T.T., Vol. MTT-16, No. 9, September 1968.

VITA

Mr. Dennis Eugene White was born on December 22, 1949 in Allentown, Pennsylvania. He did his undergraduate work at Lehigh University, receiving the Bachelor of Science degree in Electrical Engineering in 1970.

His professional experience includes work with Western Electric Company, Allentown, Pennsylvania in 1969 and with the U.S. Naval Research Laboratory, Washington, D.C. in 1971.

The author pursued his graduate studies as a teaching assistant in the Department of Electrical Engineering.